Contribution from the Department of Chemistry,
University of Virginia, Charlottesville, Virginia 29201

Relation between Structure and Magnetic Exchange Interactions in the Mixed Metal Complexes Bis(hexafluoroacetylacetonato){*N,N'*-ethylenebis[2-hydroxypropiophenone iminato-*N,O*(2−)]copper(II)}M'(II), $Cu((prp)_2en)M'(hfa)_2$, Where M' = Cu, Ni, and Mn. Crystal Structures of the Complexes ($M((prp)_2en)M'(hfa)_2$), Where M = Cu and Ni and M' = Cu, Co, and Mn

CHARLES J. O'CONNOR, DEREK P. FREYBERG, and EKK SINN*

Received August 30, 1978

The copper and nickel complexes of $(prp)_2en$ (2-hydroxypropiophenone imine) have been used as ligands to form binuclear complexes with the bis(hexafluoroacetylacetonato)metal(II) complexes $M'(hfa)_2$, where M' = copper(II), nickel(II), cobalt(II), and manganese(II). The structures of the resulting binuclear complexes $M((prp)_2en)M'(hfa)_2$ were determined from single-crystal X-ray diffraction using counter methods, and their magnetic properties were studied using high-precision magnetic susceptibility measurements in the range 4–300 K. The complexes consist of a four-coordinated metal atom M in a distorted planar environment and M' in a distorted octahedron. The extent of distortion of the planar geometry about M is approximately constant for all of the complexes, but the geometry about M' is distorted to different degrees in the different complexes, and the distortion is greatest when M' = Cu and least when M' = Mn. The complexes with $Cu((prp)_2en)$ exhibited antiferromagnetic exchange interactions, while the complexes with $Ni((prp)_2en)$ are essentially magnetically normal, exhibiting the expected properties of the M' ion. The structural similarity of the complexes with $Cu((prp)_2en)$ and $Ni((prp)_2en)$ therefore requires that the interactions observed in $Cu((prp)_2en)M'(hfa)_2$ are entirely intramolecular in origin. The magnetic interactions in the hfa complexes from $Cu((prp)_2en)$ are relatively weak when compared with those of analogous dimeric halide complexes; for $Cu((prp)_2en)Cu(hfa)_2$, the singlet–triplet separation, $-2J$, is 44.8 cm^{-1}, compared with 232 cm^{-1} for a typical related complex for which the main molecular change in substitution is Cl for hfa. The J values in the $Cu((prp)_2en)M'(hfa)_2$ complexes correlate with the structural features regardless of the nature of M' for the series studied. Crystal data for $Cu((prp)_2en)Cu(hfa)_2$: space group $P2_1/c$, $Z = 4$, $a = 13.702$ (3) Å, $b = 20.010$ (8) Å, $c = 12.579$ (3) Å, $\beta = 96.81$ (1)°, $V = 3424$ Å^3, $R = 4.0\%$, 3508 reflections. Crystal data for $Ni((prp)_2en)Cu(hfa)_2$: space group $P\bar{1}$, $Z = 2$, $a = 10.484$ (3) Å, $b = 12.446$ (8) Å, $c = 13.766$ (3) Å, $\alpha = 91.00$ (4)°, $\beta = 92.60$ (2)°, $\gamma = 110.73$ (4)°, $V = 1677$ Å^3, $R = 3.5\%$, 3440 reflections. Crystal data for $Cu((prp)_2en)Co(hfa)_2$: space group $P2_1/c$, $Z = 4$, $\alpha = 13.576$ (7) Å, $b = 20.281$ (7) Å, $c = 12.540$ (7) Å, $\beta = 97.99$ (5)°, $V = 3419$ Å^3, $R = 4.2\%$, 3254 reflections. Crystal data for $Ni((prp)_2en)Co(hfa)_2$: space group $P2_1/c$, $Z = 4$, $a = 13.468$ (3) Å, $b = 20.307$ (5) Å, $c = 12.587$ (2) Å, $\beta = 97.42$ (2)°, $V = 3413$ Å^3, $R = 5.6\%$, 4075 reflections. Crystal data for $Cu((prp)_2en)Mn(hfa)_2$: space group $P2_1/c$, $Z = 4$, $a = 13.511$ (6) Å, $b = 20.65$ (1) Å, $c = 12.548$ (5) Å, $\beta = 97.60$ (4)°, $V = 3470$ Å^3, $R = 4.4\%$, 2550 reflections. Crystal data for $Ni((prp)_2en)Mn(hfa)_2$: space group $P2_1/c$, $Z = 4$, $a = 13.387$ (7) Å, $b = 20.61$ (1) Å, $c = 12.605$ (5) Å, $\beta = 97.07$ (4)°, $V = 3452$ Å^3, $R = 4.6\%$, 2409 reflections.

Introduction

The use of tetradentate Schiff-base metal complexes, **1**, as

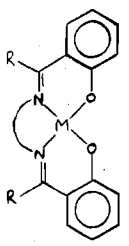

1

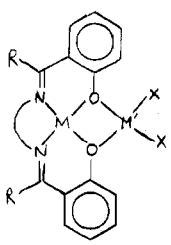

2

ligands to form binuclear complexes, **2**, has made it possible to bring pairs of similar or different metal atoms into close (ligand-bridged) proximity.[1-3] For compounds with both M and M' paramagnetic, magnetic exchange interactions have been observed. These interactions have usually been antiferromagnetic, though only the case with M = M' = Cu has been studied in detail. The ligands X may be monodentate (Cl, Br) or bidentate (NO_3, hexafluoroacetylacetone[4]). Other complexes with M = Cu and M' = Ni, Co, Fe, and Mn have only been investigated down to liquid nitrogen temperatures. Dimeric complexes of types **3**[5-7] and **4**,[8] derived from bidentate and tridentate Schiff bases, respectively, have been investigated in detail, both structurally and magnetically, and direct correlations between the structure and magnetic properties were observed. Similar nickel complexes, type **5**,[9] have also

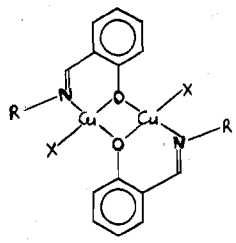

3

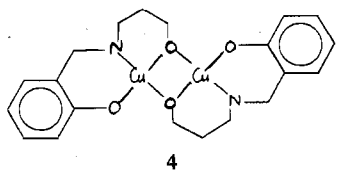

4

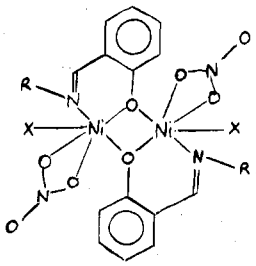

5

been characterized. All of these results involved principally four-coordinated metal atoms for copper or six-coordinated for nickel. The four-coordinated copper complexes showed increasingly strong antiferromagnetic interactions as the metal geometry approached more closely to planar. The nickel complexes were antiferromagnetic or ferromagnetic depending on the orientation of the phenolic ligand plane with respect

0020-1669/79/1318-1077$01.00/0

to the Ni_2O_2 bridging plane. The present series of complexes, type **6**, together with those of Drago et al., provides a method of studying the combination of essentially planar copper complexes with various types of octahedral transition-metal complexes.

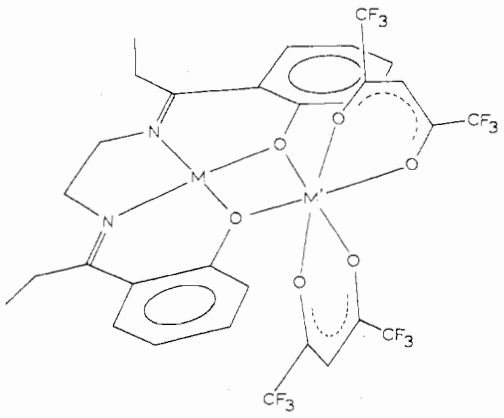

6

Experimental Section

Preparation of Complexes. 2-Hydroxypropiophenone, Hprp, and hexafluoroacetylacetone, Hhfa, were purchased from Pfaltz and Bauer, Inc., and ethylenediamine, en, was obtained from Matheson Coleman and Bell, Inc.

Metal(II) hexafluoroacetylacetonates, $M(hfa)_2$, for M = copper(II), nickel(II), cobalt(II), and manganese(II), were prepared by the methods of Cotton and Holm[10] or Walker and Li,[11] using reagent grade metal acetates.

***N,N'*-Ethylenebis(2-hydroxypropiophenone imine), $(Hprp)_2en$.** A solution of 6.0 g (40 mmol) of Hprp dissolved in 25 mL of methanol was added to a solution of 1.2 g (20 mmol) of en dissolved in 25 mL of methanol, in a 100-mL round-bottom flask fitted with a reflux condenser. The mixture was heated under reflux for 30 min, and the resulting solution of $(Hprp)_2en$ was used without separation of the ligand.

***N,N'*-Ethylenebis[2-hydroxypropiophenone iminato-*N,O*(2−)]M(II), $M(prp)_2en$ (M = Cu(II) and Ni(II)).** To a solution of 20 mmol of the metal(II) acetate dissolved in a minimum volume of hot methanol was added a solution of 20 mmol of $(Hprp)_2en$, prepared as described above. A few drops of piperidine were added, and the reaction mixture was reduced by boiling until precipitation of the $M(prp)_2en$ occurred.

{*N,N'*-Ethylenebis[2-hydroxypropiophenone iminato-*N,O*(2−)]}-{bis(hexafluoroacetylacetonato)M'(II)}, $M((prp)_2en)M'(hfa)_2$ (M = Cu(II), Ni(II), M' = Cu(II), Ni(II), Co(II), and Mn(II)). While Drago et al.[4] describe a method for the synthesis of the analogous complexes with *N,N'*-ethylenbis(salicylaldimine), salen, the method described below has been found to be better, yielding good crystals of the product without the need for recrystallization. Two millimoles (approximately 0.8 g) of $M(prp)_2en$ was dissolved in 50 mL of dichloromethane, and a solution of 2 mmol (approximately 0.95 g) of $M'(hfa)_2$ dissolved in 25 mL of methanol was added. The mixture was heated with stirring for 15 min and then allowed to cool. On cooling in a refrigerator overnight, the mixture yielded crystals of the binuclear complex. A second crop of crystals could generally be obtained by reducing the volume of the filtrate from the first crystallization, but care had to be taken to ensure that $M(prp)_2en$ did not coprecipitate.

Magnetic susceptibility measurements were made as previously described[12] using a Josephson junction magnetometer. Susceptibilities were measured in the 4–300 K temperature range at fields of 100–200 G.

Crystal densities were measured by flotation in aqueous potassium iodide containing detergent as a wetting agent.

Mass spectra of the complexes $M((prp)_2en)M'(hfa)_2$ and of the parent complexes $M(prp)_2en$ and $M'(hfa)_2$ were determined on a Hitachi Perkin-Elmer RMU-6E mass spectrometer by electron impact, using an electron beam of 70 eV.

Analyses for C, H, and N were performed by Atlantic Microlabs, Inc., and are given in Table I.[19]

Crystal Data for $Cu((prp)_2en)Cu(hfa)_2$: $Cu_2F_{12}O_6N_2C_{30}H_{24}$, mol wt 864, space group $P2_1/c$, $Z = 4$, $a = 13.702$ (3) Å, $b = 20.010$ (8) Å, $c = 12.579$ (3) Å, $\beta = 96.81$ (1)°, $V = 3424$ Å^3, $\rho_{calcd} = 1.68$ g cm^{-3}, $\rho_{obsd} = 1.67$ g cm^{-3}, μ(Mo Kα) = 14.2 cm^{-1}. Crystal dimensions (distance in mm from centroid): (100) 0.17, ($\bar{1}$00) 0.17, (011) 0.13, (0$\bar{1}\bar{1}$) 0.13, (0$\bar{1}$1) 0.11, (01$\bar{1}$) 0.11, (010) 0.06, (0$\bar{1}$0) 0.06. Maximum, minimum transmission coefficient: 0.89, 0.79.

Crystal Data for $Ni((prp)_2en)Cu(hfa)_2$: $NiCuF_{12}O_6N_2C_{30}H_{24}$, mol wt 859, space group $P\bar{1}$, $Z = 2$, $a = 10.484$ (3) Å, $b = 12.446$ (8) Å, $c = 13.766$ (3) Å, $\alpha = 91.00$ (4)°, $\beta = 92.60$ (2)°, $\gamma = 110.73$ (4)°, $V = 1677$ Å^3, $\rho_{calcd} = 1.72$ g cm^{-3}, $\rho_{obsd} = 1.68$ g cm^{-3}, μ(Mo Kα) = 13.6 cm^{-1}. Crystal dimensions (mm from centroid): (100) 0.25, (110) 0.20, ($\bar{1}\bar{1}$0) 0.20, (1$\bar{1}$0) 0.10, ($\bar{1}$10) 0.20, (011) 0.20, (001) 0.06, (00$\bar{1}$) 0.06. Maximum, minimum transmission coefficient: 0.89, 0.83.

Crystal Data for $Cu((prp)_2en)Co(hfa)_2$: $CuCoF_{12}O_6N_2C_{30}H_{24}$, mol wt 859, space group $P2_1/c$, $Z = 4$, $a = 13.576$ (7) Å, $b = 20.281$ (7) Å, $c = 12.540$ (7) Å, $\beta = 97.99$ (5)°, $V = 3419$ Å^3, $\rho_{calcd} = 1.67$ g cm^{-3}, $\rho_{obsd} = 1.66$ g cm^{-3}, μ(Mo Kα) = 12.6 cm^{-1}. Crystal dimensions (mm from centroid): (301) 0.10, ($\bar{1}\bar{1}$0) 0.11, ($\bar{1}$10) 0.11, ($\bar{1}\bar{1}$1) 0.11, ($\bar{1}\bar{1}\bar{1}$) 0.11, ($\bar{1}$11) 0.11, ($\bar{1}$1$\bar{1}$) 0.11, (010) 0.05, (0$\bar{1}$0) 0.05, (011) 0.08, (0$\bar{1}\bar{1}$) 0.08, (01$\bar{1}$) 0.08, (0$\bar{1}$1) 0.08. Maximum, minimum transmission coefficient: 0.90, 0.83.

Crystal Data for $Ni((prp)_2en)Co(hfa)_2$: $NiCoF_{12}O_6N_2C_{30}H_{24}$, mol wt 854, space group $P2_1/c$, $Z = 4$, $a = 13.468$ (3) Å, $b = 20.307$ (5) Å, $c = 12.587$ (2) Å, $\beta = 97.42$ (2)°, $V = 3413$ Å^3, $\rho_{calcd} = 1.67$ g cm^{-3}, $\rho_{obsd} = 1.66$ g cm^{-3}, μ(Mo Kα) = 11.8 cm^{-1}. Crystal dimensions (mm from centroid): (100) 0.38, ($\bar{1}$00) 0.38, (110) 0.33, (010) 0.12, (0$\bar{1}$0) 0.12, (011) 0.19, (0$\bar{1}\bar{1}$) 0.19, (01$\bar{1}$) 0.19, (0$\bar{1}$1) 0.19. Maximum, minimum transmission coefficient: 0.83, 0.73.

Crystal Data for $Cu((prp)_2en)Mn(hfa)_2$: $CuMnF_{12}O_6N_2C_{30}H_{24}$, mol wt 855, space group $P2_1/c$, $Z = 4$, $a = 13.511$ (6) Å, $b = 20.65$ (1) Å, $c = 12.548$ (5) Å, $\beta = 97.60$ (4)°, $V = 3470$ Å^3, $\rho_{calcd} = 1.66$ g cm^{-3}, $\rho_{obsd} = 1.63$ g cm^{-3}, μ(Mo Kα) = 11.6 cm^{-1}. Crystal dimensions (mm from centroid): (100) 0.17, ($\bar{1}$00) 0.17, (010) 0.065, (0$\bar{1}$0) 0.065, (011) 0.10, (0$\bar{1}\bar{1}$) 0.10, (01$\bar{1}$) 0.08, (011) 0.08. Maximum, minimum transmission coefficient: 0.91, 0.87.

Crystal Data for $Ni((prp)_2en)Mn(hfa)_2$: $NiMnF_{12}O_6N_2C_{30}H_{24}$, mol wt 850, space group $P2_1/c$, $Z = 4$, $a = 13.387$ (7) Å, $b = 20.61$ (1) Å, $c = 12.605$ (5) Å, $\beta = 97.07$ (4)°, $V = 3452$ Å^3, $\rho_{calcd} = 1.65$ g cm^{-3}, $\rho_{obsd} = 1.62$ g cm^{-3}, μ(Mo Kα) = 10.6 cm^{-1}. Crystal dimensions (mm from centroid): ($\bar{1}$00) 0.17, (110) 0.16, (1$\bar{1}$0) 0.16, (111) 0.14, (11$\bar{1}$) 0.13, (1$\bar{1}$1) 0.14, (1$\bar{1}\bar{1}$) 0.13, (010) 0.045, (0$\bar{1}$0) 0.045, (011) 0.07, (0$\bar{1}\bar{1}$) 0.07, (01$\bar{1}$) 0.07, (0$\bar{1}$1) 0.07. Maximum, minimum transmission coefficient: 0.94, 0.90.

For each crystal the Enraf-Nonius program SEARCH was used to obtain 15 accurately centered reflections which were then used in the program INDEX to obtain approximate cell dimensions and an orientation matrix for data collection. Refined cell dimensions and their estimated standard deviations were obtained from least-squares refinement of 28 accurately centered reflections. The mosaicity of the crystal was examined by the ω-scan technique and judged to be satisfactory.

Collection and Reduction of Data. Diffraction data were collected at 292 K on an Enraf-Nonius four-circle CAD-4 diffractometer controlled by a PDP8/M computer, using Mo Kα radiation from a highly oriented graphite crystal monochromator. The θ–2θ scan technique was used to record the intensities for all nonequivalent reflections for which $1° < 2\theta < 45°$ for $Ni((prp)_2en)Cu(hfa)_2$ and $Ni((prp)_2en)Mn(hfa)_2$, $1° < 2\theta < 46°$ for $Cu((prp)_2en)Cu(hfa)_2$, $Cu((prp)_2en)Co(hfa)_2$, and $Cu((prp)_2en)Mn(hfa)_2$, and $1° < 2\theta < 48°$ for $Ni((prp)_2en)Co(hfa)_2$. Scan widths (SW) were calculated from the formula $SW = A + B \tan\theta$, where A is estimated from the mosaicity of the crystals and B allows for the increase in width of the peak due to $K\alpha_1$–$K\alpha_2$ splitting. The values of A and B were respectively 0.50 and 0.30 for $Ni((prp)_2en)Cu(hfa)_2$ and $Cu((prp)_2en)Co(hfa)_2$, 0.60 and 0.30 for $Cu((prp)_2en)Cu(hfa)_2$ and $Ni((prp)_2en)Mn(hfa)_2$, and 0.70 and 0.30 for $Ni((prp)_2en)Co(hfa)_2$ and $Cu((prp)_2en)Mn(hfa)_2$. The calculated scan angle is extended at each side by 25% for background determination (BG1 and BG2). The net count is then calculated as $NC = TOT - 2(BG1 + BG2)$, where TOT is the integrated peak intensity. Reflection data were considered insignificant if intensities registered less than 10 counts above background on a rapid prescan, such reflections being automatically rejected by the computer.

The intensities of four standard reflections, monitored at 100-reflection intervals, showed no greater fluctuations during the data collections than those expected from Poisson statistics. The raw intensity data were first corrected for Lorentz–polarization effects

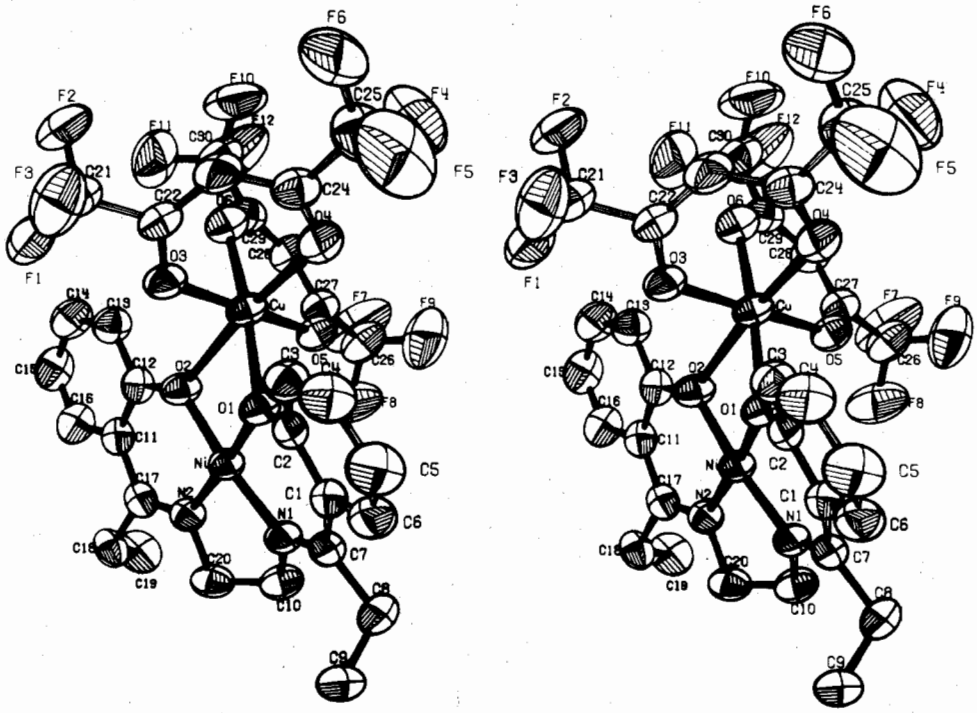

Figure 1. Stereopair view of Ni((prp)$_2$en)Cu(hfa)$_2$.

(including the polarization effect of the crystal monochromator) and then for absorption. Of the 4865 independent intensities recorded for Cu((prp)$_2$en)Cu(hfa)$_2$, 4378 for Ni((prp)$_2$en)Cu(hfa)$_2$, 4370 for Cu((prp)$_2$en)Co(hfa)$_2$, 4949 for Ni((prp)$_2$en)Co(hfa)$_2$, 5046 for Cu((prp)$_2$en)Mn(hfa)$_2$, and 3356 for Ni((prp)$_2$en)Mn(hfa)$_2$, 3508, 3440, 3254, 4075, 2550, and 2409, respectively, had $F_o^2 > 3\sigma(F_o^2)$, where $\sigma(F_o^2)$ was estimated from counting statistics.[13] These data were used in the final refinement of the structural parameters.

Determination and Refinement of the Structures. Ni((prp)$_2$en)-Cu(hfa)$_2$. The positions of the metal atoms and four of the ligand atoms were determined from a three-dimensional Patterson function calculated from all intensity data.

Cu((prp)$_2$en)Cu(hfa)$_2$. The positions of the metal and the ligand atoms were located from MULTAN IV.[14]

Full-matrix least-squares refinement was based on F, and the function minimized was $\sum w(|F_o| - |F_c|)^2$, where $|F_o|$ and $|F_c|$ are the observed and calculated structure factor amplitudes. The weights w were then taken as $[2F_o/\sigma(F_o^2)]^2$. The atomic scattering factors for nonhydrogen atoms were taken from Cromer and Waber,[15] and those for hydrogen from Stewart et al.[16] The effects of anomalous dispersion for all nonhydrogen atoms were included in F_c by using the values of Cromer and Ibers[17] for $\Delta f'$ and $\Delta f''$. Agreement factors are defined as $R = \sum||F_o| - |F_c||/\sum|F_o|$ and $R_w = (\sum w(|F_o| - |F_c|)^2/\sum w|F_o|^2)^{1/2}$. The principal programs used have been described.[18]

The positions of the atoms located from the Patterson synthesis and MULTAN phased the reflections sufficiently well to enable location of the remaining nonhydrogen atoms. In both complexes, some of the CF_3 groups exhibited positional disorder, consisting essentially of a rotation of the group by 45° around the C–C bond. This positional disorder was included in the calculation and refined.

Anisotropic temperature factors were introduced for the nonhydrogen atoms. After refinement, Fourier difference synthesis permitted location of non-methyl and some of the methyl hydrogen atoms, which were included for three cycles of full-matrix least-squares refinement and subsequently held fixed. The model converged with $R = 4.0$, $R_w = 5.0\%$ for Cu((prp)$_2$en)Cu(hfa)$_2$ and $R = 3.5$, $R_w = 4.5\%$ for Ni((prp)$_2$en)Cu(hfa)$_2$. The parameter shifts at convergence were less than one-tenth of their estimated standard deviations. The error in an observation of unit weight is 2.2 for Cu((prp)$_2$en)Cu(hfa)$_2$ and 2.1 for Ni((prp)$_2$en)Cu(hfa)$_2$.

The remaining compounds are approximately isomorphous with Cu((prp)$_2$en)Cu(hfa)$_2$. For each of these compounds, the positions of the atomic parameters from Cu((prp)$_2$en)Cu(hfa)$_2$ were used as starting values, and the refinement was completed as described above in each case. The models converged with $R = 4.2$, $R_w = 4.4\%$ for Cu((prp)$_2$en)Co(hfa)$_2$, $R = 5.6$, $R_w = 7.6\%$ for Ni((prp)$_2$en)Co(hfa)$_2$, $R = 4.4$, $R_w = 5.3\%$ for Cu((prp)$_2$en)Mn(hfa)$_2$, and $R = 4.6$, $R_w = 5.2\%$ for Ni((prp)$_2$en)Mn(hfa)$_2$. The error in an observation of unit weight is 1.7, 3.1, 2.0, and 1.9 for the compounds, respectively. The structure factor calculation with all observed and unobserved reflections included (no refinement) gave $R = 5.5$, 4.3, 7.5, 6.2, 5.6, and 5.2%, respectively, for the six compounds: on this basis it was decided that careful measurement of reflections rejected automatically by the computer during data collection would not significantly improve the results. Final Fourier difference synthesis were featureless. Tables of the observed and calculated structure factors are available.[19]

Results and Discussion

Mass spectra provide the most facile method of identification of the nature of the complexes, i.e., which metal is bonded to the Schiff base and which is bonded to hexafluoroacetylacetone. Additional confirmation is given by the order of appearance of the mass spectral peaks after the sample is introduced into the spectrometer chamber. The peaks corresponding to hexafluoroacetylacetonate appear first at comparatively low temperatures (180–200 °C), while the peaks corresponding to the Schiff base half of the complex appear only at higher (210–250 °C) temperatures.

The monoisotopic mass spectral peaks for the compounds are listed in Table II.[19] No peak is observed corresponding to the binuclear complexes, indicating their instability under the low-pressure, high-temperature conditions within the spectrometer. The fragmentation patterns observed correlate well with those of the starting metal(II) hexafluoroacetylacetonates and of the complexes of copper(II) and nickel(II) with salen, *N*,*N*′-ethylenebis(salicylaldimine).

Table IIIa contains the final positional parameters. Positional and thermal parameters are given in Table IIIb.[19] Tables IV[19] and V[19] contain the bond lengths and angles. The digits in parentheses in the tables are the estimated standard deviations in the least significant figures quoted and were derived from the inverse matrix in the course of least-squares refinement calculations. Least-squares planes data are available.[19] Figure 1 shows the stereopair view of the Ni((prp)$_2$en)Cu(hfa)$_2$ complex, and Figure 2, the Cu((prp)$_2$en)Co(hfa)$_2$ complex.

Table IIIa. Positional Parameters and Their Estimated Standard Deviations

$Cu((prp)_2en)Cu(hfa)_2$				$Ni((prp)_2en)Cu(hfa)_2$			
atom	*x*	*y*	*z*	atom	*x*	*y*	*z*
Cu(1)	0.29101 (5)	0.51612 (3)	0.46809 (4)	Cu	0.26838 (4)	0.25941 (4)	0.25810 (3)
Cu(2)	0.23438 (5)	0.48466 (3)	0.23300 (4)	Ni	0.16932 (5)	0.22589 (4)	0.04050 (3)
F(1)	0.3931 (5)	0.2976 (4)	0.1271 (6)	F(1)	0.2333 (3)	−0.0904 (2)	0.3382 (2)
F(2)	0.2840 (6)	0.2623 (3)	0.0258 (7)	F(2)	0.3327 (3)	−0.0343 (2)	0.4776 (2)
F(3)	0.3668 (7)	0.3534 (6)	−0.0134 (7)	F(3)	0.4456 (3)	−0.0527 (2)	0.3604 (3)
F(1′)	0.2944 (6)	0.2931 (5)	−0.0260 (6)	F(4)	0.6300 (5)	0.4866 (4)	0.4742 (5)
F(2′)	0.4089 (6)	0.3364 (5)	0.0767 (8)	F(5)	0.7500 (5)	0.4081 (6)	0.4108 (5)
F(3′)	0.3315 (9)	0.2665 (5)	0.1498 (12)	F(6)	0.6572 (6)	0.3460 (6)	0.5405 (4)
F(4)	−0.0314 (3)	0.3560 (2)	−0.0461 (3)	F(7)	−0.0139 (3)	0.5287 (3)	0.2732 (3)
F(5)	−0.0779 (3)	0.4424 (2)	0.0237 (4)	F(8)	0.0572 (3)	0.4905 (3)	0.1430 (2)
F(6)	−0.0683 (3)	0.3531 (2)	0.1097 (4)	F(9)	0.1911 (3)	0.6123 (2)	0.2385 (3)
F(7)	0.2267 (4)	0.7459 (2)	0.2579 (4)	F(10)	0.1396 (9)	0.2928 (9)	0.5858 (5)
F(8)	0.2208 (5)	0.6867 (2)	0.3951 (3)	F(11)	0.0027 (7)	0.1376 (5)	0.5195 (5)
F(9)	0.0989 (3)	0.6989 (2)	0.2866 (4)	F(12)	−0.0659 (6)	0.2748 (5)	0.5290 (5)
F(10)	0.4315 (5)	0.5687 (5)	−0.0065 (6)	F(4′)	0.7098 (9)	0.4657 (9)	0.3980 (9)
F(11)	0.2960 (6)	0.5646 (4)	−0.0957 (4)	F(5′)	0.6065 (11)	0.4423 (12)	0.5158 (7)
F(12)	0.3528 (7)	0.6559 (4)	−0.0427 (5)	F(6′)	0.7234 (7)	0.3457 (8)	0.4819 (9)
F(10′)	0.4134 (7)	0.6408 (6)	0.0060 (7)	F(10′)	−0.0002 (8)	0.3271 (7)	0.5519 (4)
F(11′)	0.2884 (8)	0.6234 (6)	−0.0902 (6)	F(11′)	0.1323 (8)	0.2524 (8)	0.5807 (5)
F(12′)	0.3904 (9)	0.5478 (5)	−0.0494 (7)	F(12′)	−0.0395 (10)	0.1607 (8)	0.5035 (6)
O(1)	0.2120 (3)	0.4545 (2)	0.3800 (2)	O(1)	0.3298 (2)	0.2646 (2)	0.1159 (2)
O(2)	0.3732 (2)	0.5151 (2)	0.3589 (2)	O(2)	0.0929 (2)	0.1599 (2)	0.1519 (2)
O(3)	0.2884 (2)	0.4001 (2)	0.1859 (3)	O(3)	0.2995 (3)	0.1184 (2)	0.2865 (2)
O(4)	0.0887 (3)	0.4512 (2)	0.1578 (3)	O(4)	0.4634 (3)	0.3551 (2)	0.3334 (2)
O(5)	0.1911 (3)	0.5750 (2)	0.2731 (2)	O(5)	0.2174 (2)	0.3939 (2)	0.2347 (2)
O(6)	0.2803 (3)	0.5219 (2)	0.1019 (2)	O(6)	0.1848 (3)	0.2431 (2)	0.3908 (2)
N(1)	0.1952 (3)	0.5199 (2)	0.5702 (3)	N(1)	0.2551 (3)	0.3075 (3)	−0.0649 (2)
N(2)	0.3702 (3)	0.5788 (2)	0.5562 (3)	N(2)	0.0074 (3)	0.1718 (3)	−0.0357 (2)
C(1)	0.1062 (4)	0.4210 (3)	0.5118 (4)	C(1)	0.4872 (4)	0.3432 (3)	−0.0085 (3)
C(2)	0.1513 (4)	0.4104 (2)	0.4167 (4)	C(2)	0.4541 (4)	0.2915 (3)	0.0814 (3)
C(3)	0.1304 (4)	0.3513 (3)	0.3576 (4)	C(3)	0.5559 (4)	0.2700 (4)	0.1389 (3)
C(4)	0.0660 (5)	0.3047 (3)	0.3869 (5)	C(4)	0.6882 (4)	0.3057 (4)	0.1127 (3)
C(5)	0.0207 (5)	0.3157 (3)	0.4785 (5)	C(5)	0.7245 (4)	0.3641 (4)	0.0279 (4)
C(6)	0.0401 (5)	0.3718 (3)	0.5385 (5)	C(6)	0.6253 (4)	0.3808 (4)	−0.0313 (3)
C(7)	0.1237 (4)	0.4791 (3)	0.5815 (4)	C(7)	0.3842 (4)	0.3578 (3)	−0.0779 (3)
C(8)	0.0603 (4)	0.4881 (3)	0.6717 (4)	C(8)	0.4318 (4)	0.4303 (4)	−0.1662 (3)
C(9)	0.1053 (5)	0.4511 (3)	0.7744 (4)	C(9)	0.4438 (5)	0.3577 (4)	−0.2539 (3)
C(10)	0.2158 (4)	0.5804 (3)	0.6361 (4)	C(10)	0.1491 (4)	0.3189 (4)	−0.1344 (3)
C(11)	0.5007 (4)	0.5884 (3)	0.4432 (4)	C(11)	−0.1368 (4)	0.0605 (3)	0.0866 (3)
C(12)	0.4561 (4)	0.5483 (3)	0.3578 (4)	C(12)	−0.0360 (4)	0.0941 (3)	0.1633 (3)
C(13)	0.5041 (4)	0.5427 (3)	0.2637 (4)	C(13)	−0.0699 (4)	0.0537 (4)	0.2574 (3)
C(14)	0.5907 (4)	0.5737 (3)	0.2545 (5)	C(14)	−0.1993 (5)	−0.0132 (4)	0.2760 (4)
C(15)	0.6352 (5)	0.6120 (3)	0.3390 (6)	C(15)	−0.3000 (4)	−0.0461 (4)	0.2010 (4)
C(16)	0.5909 (4)	0.6186 (3)	0.4300 (5)	C(16)	−0.2683 (4)	−0.0102 (4)	0.1097 (4)
C(17)	0.4574 (4)	0.6004 (3)	0.5431 (4)	C(17)	−0.1090 (4)	0.0973 (3)	−0.0130 (3)
C(18)	0.5142 (4)	0.6428 (3)	0.6304 (4)	C(18)	−0.2213 (4)	0.0446 (4)	−0.0917 (3)
C(19)	0.4919 (5)	0.7183 (3)	0.6147 (5)	C(19)	−0.3264 (4)	0.1076 (4)	−0.1022 (4)
C(20)	0.3253 (4)	0.5926 (3)	0.6554 (4)	C(20)	0.0315 (4)	0.2090 (4)	−0.1366 (3)
C(21)	0.3239 (5)	0.3178 (3)	0.0644 (6)	C(21)	0.3452 (4)	−0.0188 (4)	0.3829 (3)
C(22)	0.2497 (4)	0.3652 (3)	0.1082 (4)	C(22)	0.3736 (4)	0.1068 (3)	0.3575 (3)
C(23)	0.1541 (4)	0.3642 (3)	0.0606 (4)	C(23)	0.4751 (4)	0.1896 (4)	0.4112 (3)
C(24)	0.0804 (4)	0.4052 (3)	0.0930 (4)	C(24)	0.5148 (4)	0.3073 (4)	0.3937 (3)
C(25)	−0.0250 (4)	0.3900 (3)	0.0459 (5)	C(25)	0.6399 (5)	0.3889 (5)	0.4534 (4)
C(26)	0.1977 (5)	0.6920 (3)	0.2946 (5)	C(26)	0.0907 (4)	0.5137 (4)	0.2365 (4)
C(27)	0.2214 (4)	0.6276 (3)	0.2344 (4)	C(27)	0.1332 (4)	0.4205 (3)	0.2830 (3)
C(28)	0.2722 (4)	0.6360 (3)	0.1465 (4)	C(28)	0.0772 (4)	0.3781 (4)	0.3696 (3)
C(29)	0.2952 (4)	0.5822 (3)	0.0862 (4)	C(29)	0.1098 (4)	0.2943 (4)	0.4185 (3)
C(30)	0.3473 (5)	0.5949 (3)	−0.0153 (5)	C(30)	0.0482 (5)	0.2544 (5)	0.5153 (4)
H(3)	0.156 (0)	0.352 (0)	0.290 (0)	H(3)	0.529 (3)	0.231 (3)	0.197 (3)
H(4)	0.056 (0)	0.261 (0)	0.342 (0)	H(4)	0.753 (3)	0.287 (3)	0.153 (2)
H(5)	−0.028 (0)	0.282 (0)	0.495 (0)	H(5)	0.814 (3)	0.387 (3)	0.009 (3)
H(6)	0.018 (0)	0.374 (0)	0.609 (0)	H(81)	0.362 (3)	0.468 (3)	−0.183 (3)
H(81)	−0.007 (0)	0.473 (0)	0.652 (0)	H(82)	0.517 (3)	0.486 (3)	−0.148 (3)
H(82)	0.053 (0)	0.536 (0)	0.688 (0)	H(101)	0.128 (3)	0.380 (3)	−0.112 (3)
H(101)	0.192 (4)	0.573 (3)	0.702 (4)	H(102)	0.186 (3)	0.336 (3)	−0.196 (3)
H(102)	0.188 (4)	0.618 (3)	0.591 (4)	H(13)	0.004 (3)	0.076 (3)	0.304 (3)
H(13)	0.475 (4)	0.518 (3)	0.205 (4)	H(14)	−0.215 (3)	−0.032 (3)	0.341 (3)
H(14)	0.623 (4)	0.567 (3)	0.191 (4)	H(15)	−0.389 (3)	−0.094 (3)	0.209 (3)
H(15)	0.698 (4)	0.632 (3)	0.335 (4)	H(16)	−0.332 (3)	−0.038 (3)	0.062 (3)
H(16)	0.626 (4)	0.645 (3)	0.490 (4)	H(181)	−0.186 (3)	0.038 (3)	−0.155 (3)
H(181)	0.579 (4)	0.639 (3)	0.630 (4)	H(182)	−0.272 (3)	−0.032 (3)	−0.072 (3)
H(182)	0.494 (4)	0.632 (3)	0.696 (4)	H(201)	−0.044 (3)	0.217 (3)	−0.162 (3)
H(201)	0.341 (4)	0.643 (3)	0.682 (4)	H(202)	0.047 (3)	0.147 (3)	−0.170 (3)

Table IIIa (*Continued*)

$Cu((prp)_2en)Cu(hfa)_2$				$Ni((prp)_2en)Cu(hfa)_2$			
atom	*x*	*y*	*z*	atom	*x*	*y*	*z*
H(202)	0.355 (4)	0.565 (3)	0.706 (4)	H(23)	0.516 (3)	0.165 (3)	0.461 (3)
H(23)	0.144 (4)	0.332 (3)	0.012 (4)	H(28)	0.018 (3)	0.408 (3)	0.393 (3)
H(28)	0.297 (4)	0.679 (3)	0.130 (4)	H(91)	0.472 (4)	0.407 (3)	−0.306 (3)
				H(92)	0.351 (4)	0.292 (3)	−0.282 (3)
				H(93)	0.505 (4)	0.324 (3)	−0.242 (3)
$Cu((prp)_2en)Co(hfa)_2$				$Ni((prp)_2en)Co(hfa)_2$			
atom	*x*	*y*	*z*	atom	*x*	*y*	*z*
Cu	0.28479 (7)	0.51333 (5)	0.47002 (7)	N(1)	0.28229 (5)	0.51536 (3)	0.46913 (5)
Co	0.23800 (8)	0.48253 (6)	0.23792 (8)	Co	0.23610 (5)	0.48555 (4)	0.23758 (5)
F(1)	0.4104 (7)	0.3011 (5)	0.1280 (8)	F(1)	0.4128 (6)	0.3054 (4)	0.1314 (6)
F(2)	0.2912 (8)	0.2558 (5)	0.0482 (12)	F(2)	0.2973 (6)	0.2607 (3)	0.0422 (8)
F(3)	0.3580 (10)	0.3402 (8)	−0.0272 (9)	F(3)	0.3757 (9)	0.3472 (7)	−0.0139 (8)
F(1′)	0.2950 (9)	0.2803 (6)	−0.0060 (9)	F(1′)	0.3056 (8)	0.2927 (6)	−0.0150 (7)
F(2′)	0.4153 (8)	0.3318 (7)	0.0807 (11)	F(2′)	0.4248 (6)	0.3313 (5)	0.0931 (8)
F(3′)	0.3403 (14)	0.2634 (7)	0.1711 (16)	F(3′)	0.3413 (10)	0.2662 (5)	0.1629 (12)
F(4)	−0.0286 (4)	0.3537 (3)	−0.0375 (5)	F(4)	−0.0259 (3)	0.3533 (2)	−0.0367 (4)
F(5)	−0.0696 (4)	0.4428 (3)	0.0236 (5)	F(5)	−0.0692 (3)	0.4437 (2)	0.0227 (4)
F(6)	−0.0632 (4)	0.3596 (3)	0.1196 (5)	F(6)	−0.0640 (3)	0.3592 (3)	0.1189 (4)
F(7)	0.2318 (5)	0.7444 (3)	0.2585 (5)	F(7)	0.2228 (4)	0.7471 (2)	0.2474 (4)
F(8)	0.2229 (6)	0.6869 (3)	0.3960 (4)	F(8)	0.2180 (5)	0.6900 (2)	0.3889 (4)
F(9)	0.0995 (5)	0.7009 (3)	0.2830 (5)	F(9)	0.0938 (4)	0.7022 (2)	0.2787 (4)
F(10)	0.4347 (8)	0.5809 (11)	0.0012 (10)	F(10)	0.4343 (6)	0.5765 (6)	−0.0039 (6)
F(11)	0.3077 (8)	0.5600 (6)	−0.0945 (7)	F(11)	0.2978 (6)	0.5630 (4)	−0.0996 (5)
F(12)	0.3296 (10)	0.6532 (5)	−0.0540 (7)	F(12)	0.3510 (8)	0.6571 (4)	−0.0468 (6)
F(10′)	0.3957 (9)	0.6495 (7)	−0.0037 (10)	F(10′)	0.4078 (8)	0.6462 (6)	−0.0004 (8)
F(11′)	0.2763 (11)	0.5997 (12)	−0.1023 (9)	F(11′)	0.2838 (9)	0.6155 (8)	−0.0958 (7)
F(12′)	0.4135 (10)	0.5562 (6)	−0.0314 (10)	F(12′)	0.4128 (8)	0.5541 (5)	−0.0364 (6)
O(1)	0.2070 (4)	0.4502 (2)	0.3860 (4)	O(1)	0.2067 (3)	0.4542 (2)	0.3862 (3)
O(2)	0.3636 (3)	0.5106 (2)	0.3566 (3)	O(2)	0.3593 (3)	0.5118 (2)	0.3589 (3)
O(3)	0.3006 (4)	0.3984 (2)	0.1884 (4)	O(3)	0.3016 (3)	0.4008 (2)	0.1906 (3)
O(4)	0.1008 (3)	0.4511 (2)	0.1595 (4)	O(4)	0.1005 (3)	0.4521 (2)	0.1608 (3)
O(5)	0.1888 (4)	0.5772 (2)	0.2723 (4)	O(5)	0.1848 (3)	0.5799 (2)	0.2671 (3)
O(6)	0.2813 (4)	0.5234 (3)	0.1007 (4)	O(6)	0.2802 (3)	0.5250 (2)	0.1002 (3)
N(1)	0.1915 (4)	0.5181 (3)	0.5731 (5)	N(1)	0.1931 (3)	0.5186 (2)	0.5704 (3)
N(2)	0.3646 (5)	0.5777 (3)	0.5520 (5)	N(2)	0.3632 (3)	0.5760 (2)	0.5497 (3)
C(1)	0.1028 (6)	0.4190 (4)	0.5182 (6)	C(1)	0.1046 (4)	0.4187 (3)	0.5185 (4)
C(2)	0.1461 (6)	0.4071 (4)	0.4217 (6)	C(2)	0.1482 (4)	0.4089 (3)	0.4228 (4)
C(3)	0.1245 (6)	0.3500 (4)	0.3626 (6)	C(3)	0.1304 (5)	0.3506 (3)	0.3636 (4)
C(4)	0.0613 (7)	0.3039 (4)	0.3957 (7)	C(4)	0.0670 (5)	0.3036 (3)	0.3934 (5)
C(5)	0.0162 (6)	0.3166 (5)	0.4886 (8)	C(5)	0.0221 (5)	0.3139 (3)	0.4896 (6)
C(6)	0.0364 (6)	0.3715 (4)	0.5463 (7)	C(6)	0.0395 (5)	0.3686 (3)	0.5472 (5)
C(7)	0.1203 (5)	0.4773 (4)	0.5861 (6)	C(7)	0.1220 (4)	0.4776 (3)	0.5853 (4)
C(8)	0.0580 (6)	0.4863 (4)	0.6765 (7)	C(8)	0.0575 (4)	0.4872 (3)	0.6735 (5)
C(9)	0.1057 (7)	0.4510 (5)	0.7815 (6)	C(9)	0.1049 (6)	0.4536 (4)	0.7780 (5)
C(10)	0.2112 (6)	0.5779 (4)	0.6357 (6)	C(10)	0.2104 (5)	0.5799 (3)	0.6323 (4)
C(11)	0.4930 (5)	0.5847 (4)	0.4367 (6)	C(11)	0.4911 (4)	0.5853 (3)	0.4323 (4)
C(12)	0.4479 (5)	0.5438 (4)	0.3530 (6)	C(12)	0.4448 (4)	0.5439 (3)	0.3517 (4)
C(13)	0.4943 (6)	0.5350 (4)	0.2610 (6)	C(13)	0.4907 (4)	0.5339 (3)	0.2597 (5)
C(14)	0.5831 (6)	0.5664 (4)	0.2497 (7)	C(14)	0.5772 (4)	0.5660 (3)	0.2452 (5)
C(15)	0.6273 (6)	0.6070 (4)	0.3318 (8)	C(15)	0.6243 (5)	0.6062 (3)	0.3228 (5)
C(16)	0.5848 (6)	0.6142 (4)	0.4221 (7)	C(16)	0.5828 (4)	0.6160 (3)	0.4151 (5)
C(17)	0.4515 (6)	0.6002 (4)	0.5381 (6)	C(17)	0.4509 (4)	0.5985 (3)	0.5336 (4)
C(18)	0.5094 (6)	0.6439 (4)	0.6211 (7)	C(18)	0.5085 (5)	0.6408 (3)	0.6175 (5)
C(19)	0.4825 (8)	0.7182 (4)	0.6007 (8)	C(19)	0.4836 (6)	0.7148 (3)	0.5995 (6)
C(20)	0.3231 (6)	0.5933 (4)	0.6523 (6)	C(20)	0.3220 (5)	0.5929 (3)	0.6500 (4)
C(21)	0.3309 (7)	0.3126 (5)	0.0707 (9)	C(21)	0.3341 (5)	0.3148 (4)	0.0760 (7)
C(22)	0.2606 (6)	0.3632 (4)	0.1133 (7)	C(22)	0.2609 (4)	0.3643 (3)	0.1140 (4)
C(23)	0.1618 (6)	0.3610 (4)	0.0659 (6)	C(23)	0.1636 (4)	0.3625 (3)	0.0673 (4)
C(24)	0.0910 (6)	0.4041 (4)	0.0949 (6)	C(24)	0.0906 (4)	0.4052 (3)	0.0953 (4)
C(25)	−0.0185 (6)	0.3898 (4)	0.0529 (7)	C(25)	−0.0176 (4)	0.3917 (3)	0.0499 (5)
C(26)	0.1986 (7)	0.6914 (4)	0.2937 (8)	C(26)	0.1918 (5)	0.6946 (3)	0.2839 (5)
C(27)	0.2197 (6)	0.6293 (4)	0.2330 (6)	C(27)	0.2168 (4)	0.6311 (3)	0.2284 (4)
C(28)	0.2704 (6)	0.6361 (4)	0.1453 (6)	C(28)	0.2709 (4)	0.6382 (3)	0.1408 (4)
C(29)	0.2955 (6)	0.5831 (4)	0.0841 (6)	C(29)	0.2943 (4)	0.5843 (3)	0.0822 (4)
C(30)	0.3449 (7)	0.5958 (4)	−0.0157 (7)	C(30)	0.3460 (5)	0.5964 (4)	−0.0185 (5)
H(3)	0.155 (6)	0.340 (4)	0.293 (7)	H(3)	0.169 (6)	0.334 (4)	0.283 (6)
H(4)	0.038 (6)	0.272 (4)	0.350 (7)	H(4)	0.034 (6)	0.273 (4)	0.354 (6)
H(5)	−0.021 (6)	0.283 (4)	0.504 (7)	H(5)	−0.013 (6)	0.280 (4)	0.501 (6)
H(6)	0.021 (7)	0.384 (4)	0.631 (7)	H(6)	0.032 (6)	0.387 (4)	0.636 (6)
H(81)	−0.015 (6)	0.465 (4)	0.653 (7)	H(81)	−0.015 (6)	0.464 (4)	0.651 (6)

Table IIIa (*Continued*)

Cu((prp)$_2$en)Co(hfa)$_2$				Ni((prp)$_2$en)Co(hfa)$_2$			
atom	*x*	*y*	*z*	atom	*x*	*y*	*z*
H(82)	0.043 (6)	0.527 (4)	0.679 (6)	H(82)	0.037 (6)	0.528 (4)	0.670 (6)
H(101)	0.182 (6)	0.580 (4)	0.698 (7)	H(101)	0.188 (6)	0.580 (4)	0.686 (6)
H(102)	0.197 (6)	0.622 (4)	0.598 (7)	H(102)	0.197 (6)	0.631 (4)	0.602 (6)
H(13)	0.464 (6)	0.508 (4)	0.214 (6)	H(13)	0.473 (6)	0.518 (4)	0.218 (6)
H(14)	0.614 (6)	0.559 (4)	0.192 (6)	H(14)	0.615 (6)	0.555 (4)	0.203 (6)
H(15)	0.694 (6)	0.625 (4)	0.327 (7)	H(15)	0.695 (6)	0.628 (4)	0.332 (6)
H(16)	0.613 (6)	0.644 (4)	0.478 (7)	H(16)	0.616 (6)	0.649 (4)	0.472 (6)
H(181)	0.572 (6)	0.643 (4)	0.624 (7)	H(181)	0.560 (6)	0.645 (4)	0.633 (6)
H(182)	0.499 (6)	0.631 (4)	0.688 (7)	H(182)	0.490 (6)	0.639 (4)	0.703 (6)
H(201)	0.336 (6)	0.652 (4)	0.684 (7)	H(201)	0.348 (6)	0.661 (4)	0.689 (6)
H(202)	0.344 (6)	0.574 (4)	0.702 (6)	H(202)	0.354 (6)	0.585 (4)	0.706 (6)
H(23)	0.145 (6)	0.330 (4)	0.009 (6)	H(23)	0.146 (6)	0.328 (4)	0.003 (6)
H(28)	0.282 (6)	0.680 (4)	0.106 (6)	H(28)	0.282 (6)	0.685 (4)	0.086 (6)
Cu((prp)$_2$en)Mn(hfa)$_2$				Ni((prp)$_2$en)Mn(hfa)$_2$			
atom	*x*	*y*	*z*	atom	*x*	*y*	*z*
Cu	0.28448 (7)	0.51306 (4)	0.47222 (6)	Ni	0.28246 (8)	0.51449 (5)	0.47164 (7)
Mn	0.23863 (8)	0.48287 (5)	0.23392 (8)	Mn	0.23740 (9)	0.48574 (6)	0.23444 (9)
F(1)	0.4089 (7)	0.2985 (4)	0.1205 (8)	F(1)	0.4155 (8)	0.3008 (5)	0.1231 (8)
F(2)	0.2884 (8)	0.2516 (4)	0.0457 (11)	F(2)	0.2917 (9)	0.2551 (4)	0.0419 (11)
F(3)	0.3522 (9)	0.3343 (7)	−0.0376 (8)	F(3)	0.3608 (9)	0.3369 (7)	−0.0301 (9)
F(1′)	0.2866 (8)	0.2734 (6)	−0.0050 (9)	F(1′)	0.2934 (10)	0.2809 (7)	−0.0051 (12)
F(2′)	0.4140 (8)	0.3237 (7)	0.0827 (13)	F(2′)	0.4158 (9)	0.3219 (8)	0.0954 (16)
F(3′)	0.3332 (14)	0.2600 (7)	0.1665 (18)	F(3′)	0.3297 (15)	0.2609 (8)	0.1655 (20)
F(4)	−0.0341 (4)	0.3466 (3)	−0.0338 (5)	F(4)	−0.0335 (4)	0.3474 (3)	−0.0306 (5)
F(5)	−0.0702 (4)	0.4387 (3)	0.0132 (5)	F(5)	−0.0707 (4)	0.4395 (3)	0.0160 (5)
F(6)	−0.0709 (4)	0.3621 (4)	0.1196 (5)	F(6)	−0.0729 (5)	0.3635 (4)	0.1212 (6)
F(7)	0.2350 (5)	0.7454 (3)	0.2541 (5)	F(7)	0.2292 (6)	0.7478 (3)	0.2441 (5)
F(8)	0.2270 (6)	0.6890 (3)	0.3909 (4)	F(8)	0.2254 (7)	0.6927 (3)	0.3824 (5)
F(9)	0.1043 (5)	0.7034 (3)	0.2805 (5)	F(9)	0.1006 (5)	0.7054 (3)	0.2774 (6)
F(10)	0.4432 (10)	0.5906 (12)	0.0023 (11)	F(10)	0.4495 (9)	0.5883 (10)	0.0030 (10)
F(11)	0.3274 (11)	0.5589 (6)	−0.0922 (7)	F(11)	0.3274 (10)	0.5625 (7)	−0.0985 (8)
F(12)	0.3363 (11)	0.6554 (5)	−0.0601 (8)	F(12)	0.3445 (13)	0.6583 (6)	−0.0593 (9)
F(10′)	0.3987 (9)	0.6552 (6)	−0.0099 (9)	F(10′)	0.3916 (9)	0.6549 (6)	−0.0207 (10)
F(11′)	0.2911 (9)	0.5981 (8)	−0.1059 (7)	F(11′)	0.2884 (11)	0.5900 (11)	−0.1054 (8)
F(12′)	0.4318 (9)	0.5629 (6)	−0.0231 (9)	F(12′)	0.4318 (9)	0.5620 (6)	−0.0292 (9)
O(1)	0.2054 (4)	0.4508 (2)	0.3886 (3)	O(1)	0.2071 (4)	0.4536 (2)	0.3907 (4)
O(2)	0.3646 (3)	0.5101 (2)	0.3598 (3)	O(2)	0.3621 (3)	0.5103 (2)	0.3625 (3)
O(3)	0.2989 (4)	0.3955 (2)	0.1762 (4)	O(3)	0.3011 (4)	0.3980 (2)	0.1786 (4)
O(4)	0.0986 (3)	0.4464 (2)	0.1547 (4)	O(4)	0.0980 (4)	0.4475 (2)	0.1573 (4)
O(5)	0.1898 (3)	0.5815 (2)	0.2657 (4)	O(5)	0.1859 (4)	0.5845 (2)	0.2611 (4)
O(6)	0.2861 (4)	0.5281 (2)	0.0958 (3)	O(6)	0.2859 (4)	0.5290 (2)	0.0948 (4)
N(1)	0.1906 (4)	0.5180 (3)	0.5758 (4)	N(1)	0.1925 (4)	0.5174 (3)	0.5722 (4)
N(2)	0.3640 (4)	0.5771 (3)	0.5534 (4)	N(2)	0.3611 (5)	0.5747 (3)	0.5501 (4)
C(1)	0.1004 (5)	0.4206 (3)	0.5224 (5)	C(1)	0.1017 (6)	0.4199 (4)	0.5221 (6)
C(2)	0.1454 (5)	0.4088 (3)	0.4274 (5)	C(2)	0.1481 (6)	0.4099 (4)	0.4285 (6)
C(3)	0.1234 (6)	0.3515 (3)	0.3674 (6)	C(3)	0.1290 (6)	0.3533 (4)	0.3672 (6)
C(4)	0.0597 (6)	0.3070 (4)	0.3990 (6)	C(4)	0.0628 (7)	0.3065 (4)	0.3985 (7)
C(5)	0.0129 (7)	0.3188 (4)	0.4939 (7)	C(5)	0.0198 (7)	0.3170 (4)	0.4916 (8)
C(6)	0.0348 (6)	0.3735 (4)	0.5513 (6)	C(6)	0.0385 (7)	0.3714 (4)	0.5502 (7)
C(7)	0.1190 (5)	0.4782 (4)	0.5895 (5)	C(7)	0.1195 (5)	0.4775 (4)	0.5873 (6)
C(8)	0.0557 (6)	0.4879 (4)	0.6811 (6)	C(8)	0.0550 (6)	0.4878 (4)	0.6770 (6)
C(9)	0.1043 (7)	0.4549 (4)	0.7845 (6)	C(9)	0.1062 (7)	0.4546 (5)	0.7822 (6)
C(10)	0.2096 (6)	0.5782 (4)	0.6371 (6)	C(10)	0.2081 (6)	0.5779 (4)	0.6340 (6)
C(11)	0.4940 (5)	0.5836 (3)	0.4396 (5)	C(11)	0.4938 (6)	0.5849 (4)	0.4360 (6)
C(12)	0.4486 (5)	0.5434 (3)	0.3564 (5)	C(12)	0.4472 (6)	0.5436 (4)	0.3549 (6)
C(13)	0.4965 (6)	0.5349 (4)	0.2647 (6)	C(13)	0.4913 (6)	0.5331 (4)	0.2605 (6)
C(14)	0.5834 (6)	0.5658 (4)	0.2506 (6)	C(14)	0.5781 (6)	0.5657 (4)	0.2453 (7)
C(15)	0.6291 (6)	0.6059 (4)	0.3337 (7)	C(15)	0.6243 (6)	0.6059 (4)	0.3264 (8)
C(16)	0.5854 (6)	0.6132 (4)	0.4236 (6)	C(16)	0.5825 (7)	0.6147 (4)	0.4164 (7)
C(17)	0.4527 (5)	0.5982 (3)	0.5387 (5)	C(17)	0.4501 (6)	0.5971 (4)	0.5347 (6)
C(18)	0.5099 (6)	0.6404 (4)	0.6235 (6)	C(18)	0.5087 (7)	0.6408 (4)	0.6185 (7)
C(19)	0.4840 (8)	0.7142 (4)	0.6036 (7)	C(19)	0.4820 (8)	0.7135 (4)	0.5993 (8)
C(20)	0.3220 (6)	0.5921 (4)	0.6522 (6)	C(20)	0.3191 (7)	0.5910 (4)	0.6511 (6)
C(21)	0.3274 (7)	0.3089 (5)	0.0639 (8)	C(21)	0.3304 (8)	0.3102 (6)	0.0699 (9)
C(22)	0.2564 (5)	0.3586 (4)	0.1070 (6)	C(22)	0.2566 (6)	0.3602 (4)	0.1100 (7)
C(23)	0.1563 (6)	0.3557 (4)	0.0649 (6)	C(23)	0.1570 (6)	0.3574 (4)	0.0673 (7)
C(24)	0.0861 (5)	0.3989 (3)	0.0928 (5)	C(24)	0.0868 (6)	0.4004 (4)	0.0950 (6)
C(25)	−0.0224 (6)	0.3870 (4)	0.0487 (6)	C(25)	−0.0221 (6)	0.3877 (4)	0.0521 (7)
C(26)	0.2035 (7)	0.6938 (4)	0.2881 (7)	C(26)	0.1988 (8)	0.6963 (5)	0.2812 (8)
C(27)	0.2238 (6)	0.6327 (3)	0.2269 (6)	C(27)	0.2215 (6)	0.6342 (4)	0.2221 (6)
C(28)	0.2776 (6)	0.6394 (4)	0.1416 (6)	C(28)	0.2762 (6)	0.6410 (4)	0.1364 (6)

Table IIIa (*Continued*)

Cu((prp)$_2$en)Mn(hfa)$_2$				Ni((prp)$_2$en)Mn(hfa)$_2$			
atom	*x*	*y*	*z*	atom	*x*	*y*	*z*
C(29)	0.3014 (5)	0.5874 (4)	0.0823 (5)	C(29)	0.3013 (6)	0.5880 (4)	0.0795 (6)
C(30)	0.3542 (7)	0.6016 (4)	−0.0168 (6)	C(30)	0.3551 (7)	0.6014 (5)	−0.0205 (7)
H(3)	0.169 (6)	0.334 (4)	0.283 (6)	H(3)	0.163 (8)	0.345 (5)	0.300 (8)
H(4)	0.034 (6)	0.273 (4)	0.354 (6)	H(4)	0.049 (8)	0.270 (5)	0.355 (8)
H(5)	−0.013 (6)	0.280 (4)	0.501 (6)	H(5)	−0.009 (8)	0.290 (5)	0.502 (8)
H(6)	0.032 (6)	0.387 (4)	0.636 (6)	H(6)	0.029 (8)	0.374 (5)	0.615 (8)
H(81)	−0.015 (6)	0.464 (4)	0.651 (6)	H(81)	−0.029 (8)	0.473 (5)	0.639 (8)
H(82)	0.037 (6)	0.528 (4)	0.670 (6)	H(82)	0.027 (8)	0.545 (5)	0.682 (7)
H(101)	0.188 (6)	0.580 (4)	0.686 (6)	H(101)	0.180 (8)	0.580 (5)	0.706 (7)
H(102)	0.197 (6)	0.631 (4)	0.602 (6)	H(102)	0.178 (8)	0.611 (5)	0.607 (7)
H(13)	0.473 (6)	0.518 (4)	0.218 (6)	H(13)	0.450 (8)	0.499 (5)	0.202 (8)
H(14)	0.615 (6)	0.555 (4)	0.203 (6)	H(14)	0.605 (8)	0.558 (5)	0.179 (8)
H(15)	0.695 (6)	0.628 (4)	0.332 (6)	H(15)	0.684 (8)	0.632 (5)	0.314 (8)
H(16)	0.616 (6)	0.649 (4)	0.472 (6)	H(16)	0.620 (8)	0.641 (5)	0.469 (8)
H(181)	0.560 (6)	0.645 (4)	0.633 (6)	H(181)	0.556 (8)	0.632 (5)	0.602 (8)
H(182)	0.490 (6)	0.639 (4)	0.703 (6)	H(182)	0.506 (8)	0.633 (5)	0.689 (8)
H(201)	0.348 (6)	0.661 (4)	0.689 (6)	H(201)	0.346 (8)	0.642 (5)	0.667 (8)
H(202)	0.354 (6)	0.585 (4)	0.706 (6)	H(202)	0.358 (8)	0.568 (5)	0.698 (7)
H(23)	0.146 (6)	0.328 (4)	0.003 (6)	H(23)	0.148 (8)	0.327 (5)	0.014 (7)
H(28)	0.282 (6)	0.685 (4)	0.086 (6)	H(28)	0.295 (8)	0.687 (5)	0.111 (7)

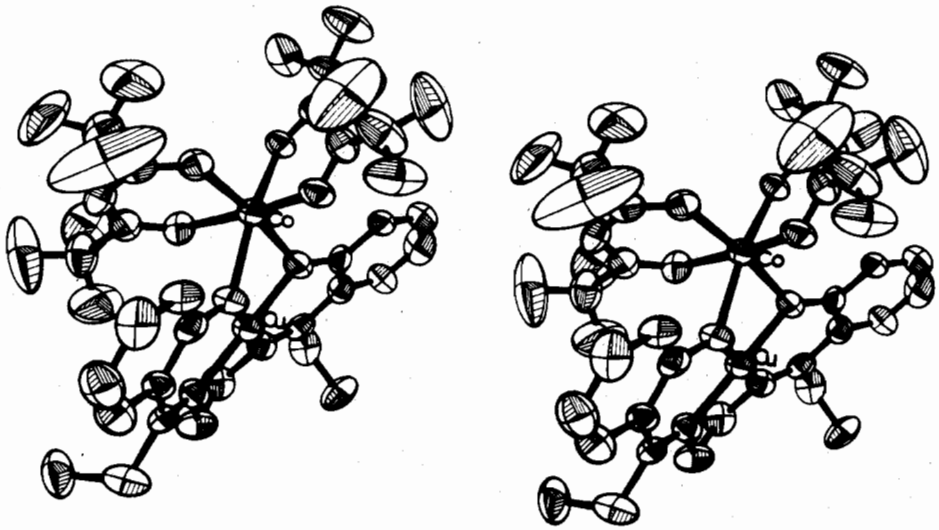

Figure 2. Stereopair view of Cu((prp)$_2$en)Co(hfa)$_2$. The atom labels are as in Figure 1. With minor differences, Figure 2 also applies to Cu((prp)$_2$en)Cu(hfa)$_2$, Cu((prp)$_2$en)Mn(hfa)$_2$, Ni((prp)$_2$en)Co(hfa)$_2$, and Ni((prp)$_2$en)Mn(hfa)$_2$.

The complexes consist of a four-coordinated metal atom M (=Cu or Ni) in a slightly distorted planar environment and M′ (=Cu, Co or Mn) in an octahedron. The planar metal group is linked to the octahedron at an edge.

(a) Cu((prp)$_2$en)Cu(hfa)$_2$. The four-coordinated copper atom is in a planar ligand environment (plane I, Table VI[19]), but the six-coordinated copper atom has highly distorted octahedral geometry as evidenced by the unevenness of the metal–ligand bond lengths. The principal distortion from regular octahedral geometry is elongation along the O(2)–Cu–O(4) axis: distances along this axis are Cu–O(2) = 2.400 (3) Å and Cu–O(4) = 2.210 (3) Å, which compare with an average distance of 1.985 Å for the other four Cu–O bond lengths. This tetragonal distortion is matched by similar, but lesser, distortion in the only other complex containing six-coordinated copper, Ni((prp)$_2$en)Cu(hfa)$_2$. Other distortion from regular symmetry is indicated by the deviation from 180° of the axes O(1)–Cu–O(6), O(2)–Cu–O(4), and O(3)–Cu–O(5) (168.8, 164.4, and 173.8°, respectively) or from the 90° angles between the three intersecting ligand planes II, O(1), O(2), O(4), and O(6), III, O(1), O(3), O(5), and O(6), and IV, O(2), O(3), O(4), and O(5) (II,III 84.3°, II,IV 86.5°, III,IV 83.5°).[19] Plane II of the octahedron shares an edge with the ligand plane (I, O(1), O(2), N(1), and N(2)) of the other copper atom, and the two planes are inclined at 38.9°. The latter angle is similar to the values observed in all of the complexes except Ni((prp)$_2$en)Cu(hfa)$_2$.

(b) Ni((prp)$_2$en)Cu(hfa)$_2$. The nickel atom is in a slightly distorted planar environment. This distortion from planarity, though slight (plane I, Table VI[19]), is greater than in any of the analogous complexes. As in the Cu((prp)$_2$en)Cu(hfa)$_2$ analogue, the six-coordinated copper environment is markedly distorted from octahedral symmetry. Again the principal distortion is tetragonal: Cu–O(2) = 2.266 (2) Å and Cu–O(4) = 2.172 (2) Å, while ⟨Cu–O⟩ = 2.006 Å for the other four metal–ligand bonds. This axial elongation along O(2)–Cu–O(4) is significantly less than in Cu((prp)$_2$en)Cu(hfa)$_2$ (a) but is still typical of six-coordinated copper(II). The axial and interplanar angles corresponding to those in (a) are 173.1, 167.7, 173.8, 88.2, 88.2, and 77.6°; all but the last of these angles indicate a closer approach to octahedral symmetry than in the complex of (a). The angle between the nickel plane (I) and the copper plane (II) with which it shares an edge is only 25.1°, which is by far the smallest value observed in any of the complexes. The average value for this angle in the other five complexes is 39.6°.

(c) Cu((prp)$_2$en)Co(hfa)$_2$. The copper atom is in a planar environment (plane I[19]) while the cobalt(II) atom is in a distorted octahedron. Although the Co–O(2) bond is elongated (2.178 (2) Å, compared with an average of 2.071 Å for the

Table VII. Coordination Spheres of the Complexes $M((prp)_2en)M'(hfa)_2$

	M, M′					
	Cu, Cu	Ni, Cu	Cu, Co	Ni, Co	Cu, Mn	Ni, Mn
⟨M′-O(2,4)⟩, Å	2.305	2.219	2.127	2.1195	2.194	2.1885
⟨M′-O(1,6)⟩, Å	1.989	2.064	2.067	2.062	2.147	2.1485
⟨M′-O(3,5)⟩, Å	1.981	1.948	2.0695	2.0705	2.1685	2.1705
⟨M′-L⟩, Å	2.092	2.077	2.089	2.084	2.170	2.170
av, Å		2.0845	2.086			2.170
(M′(O2)-M′O(4)), Å	0.190	0.094	0.137	0.105	0.084	0.087
M-M′, Å	3.032			2.963	3.037	3.035
⟨C-H⟩, Å	0.965	0.935	0.945	0.997	0.931	0.968
			av = 0.957			

other five Co–O bonds), the distortion is not tetragonal, and the approach to regular octahedral symmetry is much closer than in the complexes of (a) and (b) which contain six-coordinated copper(II). The angular distortion is significant however: the axial angles (see (a)) are 172.7, 165.3, and 170.3° instead of 180° and the interplanar angles are 85.2, 87.7, and 83.5° instead of 90°. The angle between the copper and cobalt planes that share the bridging oxygens (I and II) is 40.4°.

(d) $Ni((prp)_2en)Co(hfa)_2$. As in the $Cu((prp)_2en)Co(hfa)_2$ analogue (c), the nickel environment is planar and the octahedral cobalt environment is less distorted than in the six-coordinated copper complexes of (a) and (b). The Co–O(2) bond is again the longest (2.172 (6) Å, compared with ⟨Co–O⟩ = 2.066 Å for the other five metal–ligand bonds), and the corresponding axial and interplanar angles are 172.2, 163.3, 169.9, 85.4, 88.4, and 81.8°. The angle between the nickel and cobalt planes which share the bridging oxygens (I and II) is 38.7°.

(e) $Cu((prp)_2en)Mn(hfa)_2$. The copper atom is planar, while the octahedral manganese(II) environment is less distorted than in the complexes of (a) and (b). As with the above compounds, Mn–O(2) is the longest bond, but by a smaller margin (2.236 (3) Å, compared with ⟨Mn–O⟩ = 2.157 Å for the other metal–ligand bonds). In terms of bond lengths, the manganese environment approaches more closely to octahedral symmetry than do the six-coordinated copper(II) and cobalt(II) environments in (a)–(d). However, the angular distortion is still considerable; the axial and interplanar angles corresponding to those described above are 169.9, 162.7, 168.3, 82.0, 89.5, and 83.5°. The angle between the copper and manganese planes which share the bridging oxygens (I and II) is 40.4°.

(f) $Ni((prp)_2en)Mn(hfa)_2$. As in the $Cu((prp)_2en)Mn(hfa)_2$ analogues of (e), the nickel atom is planar and the octahedral manganese environment is much less distorted than the corresponding copper(II) environment in (a) and (b) and slightly less distorted than for cobalt(II) in (c) and (d). Again, Mn–O(2) is the longest bond, while the corresponding axial and interplanar angles are 169.9, 160.4, 167.4, 83.0, 89.9, and 81.6°. The angle between the nickel and manganese planes which share the bridging oxygens is 39.6°.

Of the six complexes, the two $M((prp)_2en)Cu(hfa)_2$ compounds differ the most markedly from the others because of the dramatic tetragonal (Jahn–Teller) distortion at the copper atom. The $M((prp)_2en)Co(hfa)_2$ and $M((prp)_2en)Mn(hfa)_2$ complexes also differ from each other due to the cobalt and manganese environments, though the differences are slighter. However, a comparison of interplanar angles and metal–ligand bond lengths and angles clearly indicates that the main differences between $Cu((prp)_2en)M'(hfa)_2$ and $Ni((prp)_2en)M'(hfa)_2$ is due to the interchange of copper and nickel metals inside the $(prp)_2en$ ligand: certain angles and bond lengths show consistent changes when nickel is substituted for copper in the Schiff-base ligand, and this substitution is therefore responsible for the change. $Ni((prp)_2en)Cu(hfa)_2$ constitutes a unique case: it differs more in structural detail than any of the other complexes, and it is also the only one which crystallizes in a different space group. Bond lengths of the coordination spheres of the complexes are in Table VII.

Table IX

Curie–Weiss Parameters for $Ni((prp)_2en)M'(hfa)_2$

M′	g	θ	α
Mn	1.96	0.02	0.0002
Co	4.58	−0.15	0.0074
Ni	2.27	−0.90	0.0004
Cu	2.18	−0.25	0.0006

Magnetic Parameters for $Cu((prp)_2en)M'(hfa)_2$

M′	g(Cu)	g(M′)	J
Mn	2.05	1.98	−13.2
Co[a]	2.05	4.58	−16.3
Ni	2.05	2.27	−48.0
Cu	2.03	2.15	−44.8

[a] A temperature-independent term of 0.0065 emu/mol was required.

It is clear that compounds containing different pairs of metals in the same ligand environment are structurally sufficiently similar to allow meaningful comparison of their magnetic properties and that the structures of the environment of the metal M′ varies less for different metals (Co, Cu, Mn) if the metal M is kept constant. It had been assumed in previous studies[20] that there was sufficient similarity between a series of binuclear and trinuclear transition-metal complexes in the same ligand environment, though there had not been direct structural evidence at the time. This is clearly valid for approximate comparisons of magnetic data, especially if comparisons are made in a series within which one of the metals (either M or M′) is kept constant and if the compounds are approximately structurally isomorphous as is the case for most members of the present series. At the same time, the importance of any structure-independent differences between strengths of interactions of different types of electron configurations can be determined.

The magnetic susceptibilities, and, where appropriate, magnetic moments of each of the complexes, are listed in Table VIII.[19] The magnetic properties of the compounds with diamagnetic nickel(II) in the square-planar position were analyzed first, $Ni((prp)_2en)M'(hfa)_2$, M′ = Cu, Ni, and Mn. The M′ ions for the most part exhibited Curie–Weiss behavior. The Curie–Weiss equation used here is

$$\chi = \frac{Ng^2\mu_B^2 S(S+1)}{3k(T+\theta)} + \alpha \qquad (1)$$

where the parameters have their usual meaning and α indicates a temperature-independent paramagnetism. The results of the least-squares fit of the data to eq 1 for $Ni((prp)_2en)M'(hfa)_2$, M′ = Mn, Ni, and Cu, are shown in Table IX. Figure 3

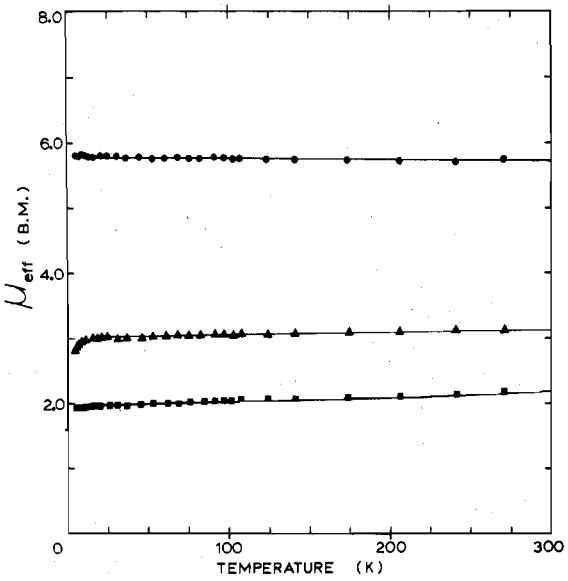

Figure 3. Effective magnetic moment as a function of temperature for Ni((prp)$_2$en)M′(hfa)$_2$: M′ = Cu (■), Ni (▲), Mn (●). The line represents the fit of the data to eq 1.

shows plots of the effective magnetic moment μ_{eff} $[(7.997\chi T)^{1/2}]$ vs. temperature, with the smooth line representing the values calculated from eq 1. As shown in the figure, the quality of the fits is quite good, and there is evidence of little deviation from theory at even the lowest temperatures obtained. The value of the TIP term is due to contribution from both the diamagnetic square-planar nickel and the paramagnetic octahedral metals. The drop in the low-temperature moment for the Ni–Ni compound is due to zero-field splitting of $S = 1$ under distorted octahedral symmetry with $|D|/k \simeq 2.3$ K.

The compounds Cu((prp)$_2$en)M′(hfa)$_2$, M′ = Cu, Ni, and Mn, presented more of a challenge in the analysis of the magnetic data. The magnetic properties of these compounds indicate the presence of antiferromagnetic exchange interactions as shown by the drop in the effective magnetic moment, μ_{eff}, in each case. The compounds with M′ = Cu and Co showed a maximum in the susceptibility while those with M′ = Mn and Ni did not. Each system had to be analyzed with equations derived for the different electronic spins on each atom. The spin Hamiltonian which best describes the magnetic properties of these systems uses the Heisenberg exchange model:

$$\mathcal{H} = -2JS_1 \cdot S_2 + g_1\mu_B H \cdot S_1 + g_2\mu_B H \cdot S_2 \qquad (2)$$

The effect of the spin Hamiltonian is to lift the zero-field spin degeneracy of the binuclear molecule due to spin–spin coupling between the two paramagnetic centers. The result is a single paramagnetic center with coupled spin states $S_T = S_2 + S_1, S_2 + S_1 - 1, \ldots, S_2 - S_1$. For the case $S_1 = {}^1/_2$, there are two resulting states, $S_T = S_2 \pm {}^1/_2$. The resulting energy levels for $S_1 = {}^1/_2$ and $S_2 = {}^1/_2$, 1, and ${}^5/_2$ are illustrated in Figure 4. The magnetic susceptibility may then be calculated by summing the magnetic moments of the energy levels over the Boltzmann distribution of the energy levels.

In the first analysis for the M = Cu, M′ = Cu system, the Bleaney–Bowers equation, eq 2, for copper dimers[21] was used. However, the fit required the addition of a paramagnetic impurity (1%) and TIP term to compensate for the finite values of the susceptibility at low temperatures. The Bleaney–Bowers equation is

$$\chi = \frac{Ng^2\mu_B^2}{kT}\frac{2e^x}{1 + 3e^x} + \alpha \qquad (3)$$

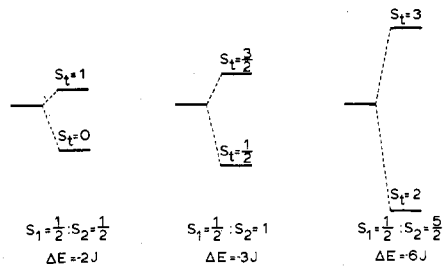

Figure 4. Energy levels for spin coupling between spins of $S_1 = {}^1/_2$ and $S_2 = {}^1/_2$, 1, and ${}^5/_2$.

where $x = 2J/kT$ and α is the temperature-independent paramagnetism.

Equation 3 assumes that the two copper ions are equivalent. Since the molecule does not have dimeric symmetry, an equation was derived using the spin Hamiltonian in eq 2 which reflected the symmetry differences of the two copper ions by including a provision for nonequal g values for M (Cu_1) and M′ (Cu_2). The equation derived from Van Vleck's formula[22] is

$$S_1 = {}^1/_2, \quad S_2 = {}^1/_2$$

$$\chi = \frac{N\mu_B^2}{2kT}\left\{\left[(g_1 + g_2)^2 + \frac{(g_1 - g_2)^2}{x}\right]e^x - \frac{(g_1 - g_2)^2}{x}\right\} \Big/ (1 + 3e^x) \qquad (4)$$

where $x = 2J/kT$, $g_1 = g(\mathrm{M})$, and $g_2 = g(\mathrm{M}')$. If we assume the dimeric limiting conditions ($g_1 = g_2$), we obtain the $S = {}^1/_2$ dimer equation shown in eq 3. The least-squares fit of the data to eq 4 still requires a 1% paramagnetic impurity correction, but the temperature-independent paramagnetism term is generated in the equation by the difference in g values and an additional term is not required.

Equations were derived in a similar fashion for the M = Cu, M′ = Ni and Mn systems with $S_1 = {}^1/_2$ and $S_2 = 1$ and ${}^5/_2$, respectively. The equations are

$$S_1 = {}^1/_2, \quad S_2 = 1$$

$$\chi = \frac{N\mu_B^2}{2kT}\left\{\left[(2g_1 + g_2)^2 + g_1^2 + \frac{2(g_1 - g_2)^2}{x}\right]e^x + g_1^2 - \frac{2(g_1 - g_2)^2}{x}\right\} \Big/ (2 + 4e^x) \qquad (5)$$

where $x = 3J/kT$, $g_1 = g(S_1)$, and $g_2 = g(S_2)$, and

$$S_1 = {}^1/_2, \quad S_2 = {}^5/_2$$

$$\chi = \frac{N\mu_B^2}{2kT}\left\{\left[(5g_1 + g_2)^2 + 20g_1^2 + \frac{5(g_1 - g_2)^2}{x}\right]e^x + 20g_1^2 - \frac{5(g_1 - g_2)^2}{x}\right\} \Big/ (5 + 7e^x) \qquad (6)$$

where $x = 6J/kT$, $g_1 = g(S_1)$, and $g_2 = g(S_2)$.

In each of the equations derived, the limiting condition of $g_1 = g_2$ simplifies the equation to the standard equations for mixed-metal binuclear exchange shown in eq 7 and 8.

$$S_1 = {}^1/_2, \quad S_2 = 1, \quad g_1 = g_2$$

$$\chi = \frac{Ng^2\mu_B^2}{2kT}\frac{10e^x + 1}{2 + 4e^x} \qquad (7)$$

$$S_1 = \tfrac{1}{2}, \quad S_2 = \tfrac{5}{2}, \quad g_1 = g_2$$

$$\chi = \frac{Ng^2\mu_B{}^2}{kT} \frac{28e^x + 10}{5 + 7e^x} \tag{8}$$

In each of the three systems exhibiting exchange interactions, M = Cu and M′ = Cu, Ni, and Mn, the theoretical predictions are closely followed by the experimental data. The data are plotted with the theoretical curves in Figures 5–7. The resulting best fit parameters are listed in Table IX.

The M = Cu, M′ = Cu susceptibility closely parallels the behavior predicted for copper dimers, but this behavior is as expected since the two g values are very similar. Neither of the compounds M = Cu, M′ = Ni or Mn shows a maximum in the susceptibility vs. temperature plots; however, they show similar behavior in moment vs. temperatures plots. The drop in effective magnetic moment may be explained by the depopulation of the excited S_T spin states. At high temperatures all spin states are populated and the system behaves as if the two magnetic centers were noninteracting. The low-temperature distribution has only the low S_T manifold populated, resulting in a lower magnetic moment when J is negative and a higher magnetic moment when J is positive.

The maximum and minimum values for the magnetic moment from eq 4 for $g = 2$ are 6.93 and 4.89. It is shown from the data plotted in Figure 6 that these values are approached on the high- and low-temperature sides, respectively, illustrating that the system encompasses the extremes of antiferromagnetic interaction in the temperature range examined here and that the two g values are close to the free-spin value.

At low temperatures and under the influence of spin–orbit coupling, the $^4T_{1g}$ ground term of octahedrally coordinated cobalt(II) splits to form a Kramers doublet ground state with an effective spin $S' = \frac{1}{2}$.[23] The analysis of the magnetic data of M((prp)$_2$en)Co(hfa)$_2$ with the $S = \frac{1}{2}$ model has met with limited success. The least-squares fit of the compound with M = Ni and M′ = Co to the Curie–Weiss equation, eq 1, with $S' = \frac{1}{2}$ gives acceptable values for the fitted parameters (Table IX) and a quantitative fit over the entire temperature range 4–100 K. The large α term is due to coupling of the ground state to the low-lying excited states of the $^4T_{1g}$ term.

The least-squares fit of the magnetic exchange interactions of the compound with M = Cu and M′ = Co using the $S_1 = \frac{1}{2}$, $S_2 = \frac{1}{2}$ model (eq 4) is illustrated in Figure 8. There is excellent agreement at temperatures equal to and above χ_{max}, but at temperatures below χ_{max} the calculated susceptibility falls off more rapidly than the experimental curve and has a lower low-temperature-limiting value. The shortcomings of the $S_1 = \frac{1}{2}$, $S_2 = \frac{1}{2}$ model in describing the behavior of the Cu–Co analogue indicate that the fitted value for the exchange parameter J is only approximate. Equation 4 assumes that the g value is isotropic for each ion, a reasonable assumption for Mn^{2+}, Ni^{2+}, and Cu^{2+}, but the g value of Co^{2+} on the other hand is very sensitive to small changes in symmetry and is often known to have a high degree of g-value anisotropy.[24]

The limited information available from powder data did not merit inclusion of additional parameters for g-value anisotropy and spin–orbit coupling. A vigorous analysis of the cobalt analogue requires single-crystal measurements to obtain the anisotropy contribution from cobalt(II) and spin–orbit coupling calculations which include the magnetic contribution from all of the levels of the $^4T_{1g}$ manifold. This will be discussed in greater detail elsewhere.[25]

Due to the orbital contribution in the Cu–Co complex, the J value obtained is not necessarily unique, and it may not be valid to group this complex with the Cu–Cu, Cu–Ni, and Cu–Mn compounds. However, no significant problem should exist with comparisons of the latter complexes.

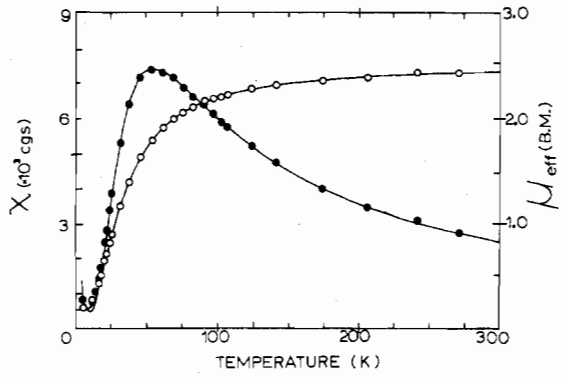

Figure 5. Magnetic susceptibility (●) and effective magnetic moment (○) plotted as a function of temperature for Cu((prp)$_2$en)Cu(hfa)$_2$. The curve represents the fit of the data to eq 4.

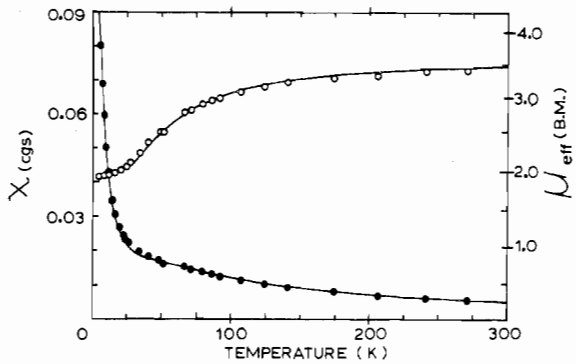

Figure 6. Magnetic susceptibility (●) and effective magnetic moment (○) plotted as a function of temperature for Cu((prp)$_2$en)Ni(hfa)$_2$. The curve represents the fit of the data to eq 5.

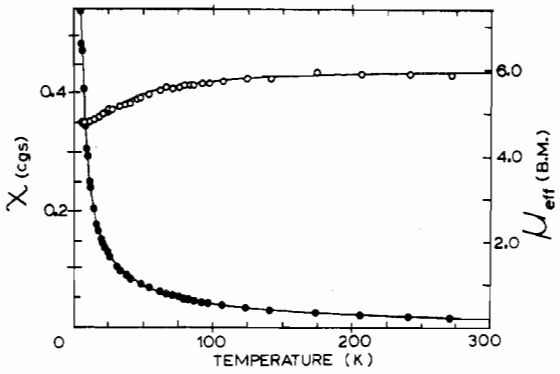

Figure 7. Magnetic susceptibility (●) and effective magnetic moment (○) plotted as a function of temperature for Cu((prp)$_2$en)Mn(hfa)$_2$. The curve represents the fit of the data to eq 6.

Correlations have previously been demonstrated between strengths of antiferromagnetic interactions and various structural features. These structural features include distortion from planar toward tetrahedral stereochemistry in four-coordinated transition-metal ions,[2,6–8] decrease in the M–O–M′ bridging angles,[2,26–32] weakening of one of the metal–oxygen bonds in the M–O–M′ bridge,[31,33] and the deviation from coplanarity of the principal ligand planes of the two interacting metals.[33] These correlations have been examined in a variety of binuclear complexes containing identical metal atoms, usually copper(II), in the same environment, but no such study has been carried out for dissimilar metal atoms. The J values are largest for copper and nickel and smaller for manganese and cobalt. To account for this, we examined each of the available structure factors known to affect strengths and signs of magnetic exchange interactions.

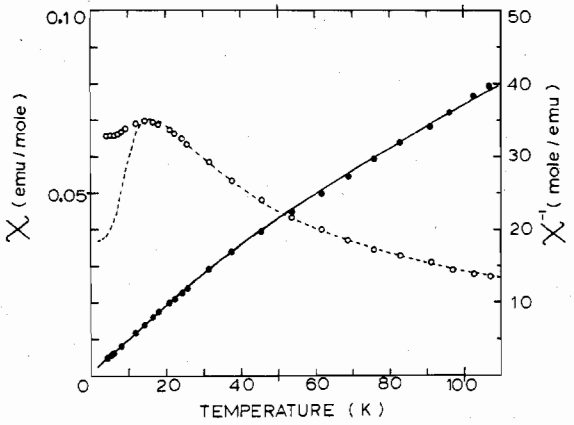

Figure 8. Magnetic susceptibility of Cu((prp)$_2$en)Co(hfa)$_2$ (○) and inverse magnetic susceptibility of Ni((prp)$_2$en)Co(hfa)$_2$ (●) plotted as a function of temperature. Fitted curves were obtained as described in text.

Table X

	M, M′					
	Cu, Cu	Cu, Co	Cu, Mn	Ni, Cu	Ni, Co	Ni, Mn
M-O(1)-M′,[a] deg	101.7	96.8	96.9	104.0	98.5	98.3
M-O(2)-M′, deg	89.4	92.9	94.5	97.6	94.9	95.8
⟨M-O-M′⟩, deg	95.5$_5$	94.85	95.7	100.8	96.7	97.0$_5$

[a] As M-O-M′ increases, J becomes more antiferromagnetic.

The copper in each of the Cu((prp)$_2$en)M′(hfa)$_2$ complexes is equally planar, within experimental error, so that the effect of distortion from planarity can reasonably be ignored due to invariance. There are differences in the M′ structure, and the effect of distortion from regular octahedral geometry has not been well studied experimentally. However, it seems unlikely that the effect of this parameter on exchange interactions would be large, and there is some preliminary experimental evidence to support this in a series of nickel(II) complexes.[9,34] The difference in coplanarity of the principal ligand planes is quite small compared to that normally required, from previous observations,[33] to cause large changes in J.

The average M–O–M′ bridging angles are the same for the Cu–Cu and the Cu–Mn complexes, so that, on a cursory analysis, the effect of the bridging angles might be dismissed in this case. However, lengthening of the metal–oxygen bonds has been shown to lead to smaller magnitudes of J values, i.e., to a diminished effect. In each of the binuclear compounds under discussion, only one of the four metal–oxygen bonds is elongated. Therefore the bridging angle with the shorter bonds, namely M–O(1)–M′, will have a greater effect, and the overall effect will be the weighted, rather than the direct, average of the two contributing angles. Thus, since one of the M–O(2) bonds is so elongated in each case, it is the M–O(1)–M′ angle that makes the major contribution to the exchange interaction. It is the existence of a strongly bonded M–O(1)–M′ angle that allows comparison between the Cu–Cu and Cu–Mn complexes at all. The bond angles under consideration are listed in Table X. There is experimental evidence that as M–O–M increases, J becomes more antiferromagnetic,[2,26-32] and our structural and magnetic data agree with this.

The Cu–O(2) bond is so weak (2.400 (3) Å) that the expected ferromagnetic contribution of the smaller Cu–O(2)–Cu bonding angle should have only a very small effect on the magnitude of the overall antiferromagnetic J value. However, the elongation of the analogous O(2)–Mn bond is much smaller so that the Cu–O(2)–Mn contribution to J should be more significant. The effect would be a reduction of the magnitude of the antiferromagnetic J value, reinforcing the effect of the smaller Cu–O(1)–Mn angle described above.

In a comparison between the Cu–Cu and Cu–Mn complexes, the magnitude of J is seen to be linked to the magnitude of the M–O(1)–M′ angle just as it was in the case of dimeric copper(II) complexes which had identical metal atoms and bridging ligand environment.[32] This result shows that it is reasonable to make the same kind of comparisons between structural and magnetic properties in complexes with dissimilar metal environments and dissimilar metals. Since the difference in the J values can be entirely accounted for by changes in structural features, it is reasonable to conclude that nonstructural differences in the compounds, such as the different d-electron configurations, are unimportant or at least less important than the structural factors. Even though it may not be valid to group Cu((prp)$_2$en)Co(hfa)$_2$ with the other two complexes, the observed low J value appears able to be rationalized in terms of the structural factors: the Cu–O(1)–Co angle is not significantly smaller than the analogous Cu–O(1)–Mn angle and cannot account for the reduction in $|J|$, but the Cu–O(2) bond is markedly shorter than its analogues in the other compounds. Thus the ferromagnetic contribution of the Cu–O(2)–Co angle is more important here, though not predominant. Its effect would be to force a reduction in the magnitude of the antiferromagnetic J value, as is observed.

The results show that a correlation between magnetic exchange and structural features is possible in unsymmetrical compounds containing similar or dissimilar metal atoms. Specifically, a relationship between J and ligand bridging angles is observed, provided that the values of unequal angles are not averaged. The conclusions are limited by the small range of compounds but are nevertheless highly informative and useful. In addition to the compounds reported here, work is underway on M = Ni(II), Cu(II), and Fe(II) and M′ = Co(II), Fe(II), and Fe(III) to investigate the behavior of iron in metal–metal exchange situations with various metal ions and to observe the effect of spin–orbit coupling on the exchange.

This series of compounds provides the first systematic investigation of single ion–binuclear interaction correlated with crystal structure and magnetic data. There is current interest in binuclear systems with nonequivalent metals because of their applications in biological systems[35] and in oxidation–reduction reactions involving electron transport bridges.[36] It is hoped that the analysis of the binuclear systems in the solid state may be used as models for the behavior of similar systems in solution.

Acknowledgment. NSF (Grant CHE77-01372) and Research Corp. support of this research is gratefully acknowledged.

Registry No. Cu(prp)$_2$en, 36820-28-7; Ni(prp)$_2$en, 28560-28-3; Cu((prp)$_2$en)Cu(hfa)$_2$, 69069-39-2; Ni((prp)$_2$en)Cu(hfa)$_2$, 69120-35-0; Cu((prp)$_2$en)Co(hfa)$_2$, 69069-40-5; Ni((prp)$_2$en)Co(hfa)$_2$, 69089-20-9; Cu((prp)$_2$en)Mn(hfa)$_2$, 69089-19-6; Ni((prp)$_2$en)Mn(hfa)$_2$, 69069-41-6; Cu(hfa)$_2$, 14781-45-4; Ni(hfa)$_2$, 14949-69-0; Co(hfa)$_2$, 19648-83-0; Mn(hfa)$_2$, 19648-86-3; (Hprp)$_2$en, 69069-32-5; Hprp, 610-99-1; en, 107-15-3; Ni((prp)$_2$en)Ni(hfa)$_2$, 69069-42-7; Cu((prp)$_2$en)Ni(hfa)$_2$, 69069-43-8.

Supplementary Material Available: Analytical results (Table I), mass spectral fragmentation patterns (Table II), positional and thermal parameters (Table IIIb), bond lengths (Table IV) and angles (Table V), selected mean planes (Table VI), magnetic susceptibilities (Table VIII), and a listing of observed and calculated structure factors (125 pages). Ordering information is given on any current masthead page.

References and Notes

(1) S. J. Gruber, C. M. Harris, and E. Sinn, *Inorg. Chem.*, 7, 268 (1968); *Inorg. Nucl. Chem. Lett.*, 3, 495 (1967); S. J. Gruber, C. M. Harris,

and E. Sinn, *J. Inorg. Nucl. Chem.*, **30**, 1805 (1968).
(2) E. Sinn and C. M. Harris, *Coord. Chem. Rev.*, **4**, 391 (1969).
(3) S. Kokot, C. M. Harris and E. Sinn, *Aust. J. Chem.*, **25**, 45 (1972).
(4) N. B. O'Bryan, T. O. Maier, I. C. Paul, and R. S. Drago, *J. Am. Chem. Soc.*, **95**, 6640 (1973).
(5) C. M. Harris and E. Sinn, *J. Inorg. Nucl. Chem.*, **30**, 2723 (1968).
(6) R. B. Coles, C. M. Harris, and E. Sinn, *Inorg. Chem.*, **8**, 2607 (1969); *Aust. J. Chem.*, **23**, 243 (1970); C. M. Harris, J. M. James, P. J. Milham, and E. Sinn, *Inorg. Chim. Acta*, **3**, 81 (1969).
(7) E. Sinn and W. T. Robinson, *J. Chem. Soc., Chem. Commun.*, 359 (1972); R. M. Countryman, W. T. Robinson, and E. Sinn, *Inorg. Chem.*, **13**, 2013 (1974); P. C. Healy, G. M. Mockler, D. P. Freyberg, and E. Sinn, *J. Chem. Soc., Dalton Trans.*, 691 (1975); R. J. Butcher and E. Sinn, *Inorg. Chem.*, **15**, 1604 (1976); E. Sinn, *Inorg. Chem.*, **15**, 366 (1976).
(8) E. Sinn, *J. Chem. Soc., Chem. Commun.*, 665 (1975); *Inorg. Chem.*, **15**, 358 (1976); J. A. Davis and E. Sinn, *J. Chem. Soc., Dalton Trans.*, 165 (1976).
(9) R. J. Butcher, J. Jasinski, G. M. Mockler, and E. Sinn, *J. Chem. Soc., Dalton Trans.*, 1099 (1976); R. J. Butcher and E. Sinn, *J. Chem. Soc., Chem. Commun.*, 832 (1975).
(10) F. A. Cotton and R. H. Holm, *J. Am. Chem. Soc.*, **82**, 2979 (1960).
(11) W. R. Walker and N. C. Li, *J. Inorg. Nucl. Chem.*, **27**, 2255 (1965).
(12) E. J. Cukauskas, B. S. Deaver, Jr., and E. Sinn, *J. Chem. Soc., Chem. Commun.*, 698 (1974); *J. Chem. Phys.*, **67**, 1257 (1977); E. J. Cukauskas, B. S. Deaver, Jr., and E. Sinn, *Bull. Am. Phys. Soc.*, **19**, 229, 1120 (1974).
(13) P. W. R. Corfield, R. J. Doedens, and J. A. Ibers, *Inorg. Chem.*, **6**, 197 (1967).
(14) G. Germain, P. Main, and M. M. Woolfson, *Acta Crystallogr., Sect. B*, **26**, 274 (1974).
(15) D. T. Cromer and J. T. Waber, "International Tables for X-Ray Crystallography", Vol. IV, Kynoch Press, Birmingham, England, 1974.
(16) R. F. Stewart, E. R. Davidson, and W. T. Simpson, *J. Chem. Phys.*, **42**, 3175 (1965).
(17) D. T. Cromer and J. A. Ibers, ref 15.
(18) G. M. Mockler, D. P. Freyberg, and E. Sinn, *J. Chem. Soc., Dalton Trans.*, 447 (1976).
(19) Supplementary material.
(20) S. J. Gruber, C. M. Harris, and E. Sinn, *J. Chem. Phys.*, **49**, 2183 (1968).
(21) B. Bleaney and K. D. Bowers, *Proc. R. Soc. London, Ser. A*, **214**, 451 (1952).
(22) J. H. Van Vleck, "Electric and Magnetic Susceptibilities", Oxford University Press, London, 1932.
(23) R. L. Carlin, C. J. O'Connor, and S. N. Bhatia, *J. Am. Chem. Soc.*, **98**, 685 (1976).
(24) J. S. Griffith, "The Theory of Transition Metal Ions", Cambridge University Press, New York, 1961, p 360.
(25) C. J. O'Connor and E. Sinn, to be submitted for publication.
(26) R. L. Martin in "New Pathways in Inorganic Chemistry", Ebsworth, Maddock, and Sharp, Eds., Cambridge University Press, London, 1968, Chapter 9.
(27) S. J. Gruber, C. M. Harris, and E. Sinn, *Inorg. Chem.*, **7**, 268 (1968).
(28) M. Kato, H. B. Jonassen, and J. C. Fanning, *Chem. Rev.*, **64**, 99 (1964), and references cited.
(29) J. Lewis and R. A. Walton, *J. Chem. Soc. A*, 1559 (1953).
(30) J. Lewis, F. E. Mabbs, and A. Richards, *J. Chem. Soc. A*, 1014 (1967); A. van den Bergen, K. S. Murray, and B. O. West, *Aust. J. Chem.*, **21**, 1517 (1968); J. D. Dunitz and L. E. Orgel, *J. Chem. Soc.*, 2594 (1953); K. S. Murray, A. van den Bergen, M. J. O'Connor, N. Rehak, and B. O. West, *Inorg. Nucl. Chem. Lett.*, **4**, 87 (1968).
(31) E. Sinn, *Coord. Chem. Rev.*, **5**, 313 (1970), and references cited.
(32) D. J. Hodgson, *Prog. Inorg. Chem.*, **19**, 173 (1975), and references cited.
(33) E. Sinn, *Inorg. Chem.*, 9, 2376 (1970); **15**, 2698 (1976); P. G. Sim and E. Sinn, to be submitted for publication.
(34) R. J. Butcher, C. J. O'Connor, and E. Sinn, to be submitted for publication.
(35) C. Seiter, to be submitted for publication; L. J. Wilson, to be submitted for publication.
(36) J. M. Malin, D. A. Ryan, and T. V. O'Halloran, *J. Am. Chem. Soc.*, **100**, 2097 (1978).

Contribution from Chemistry Departments I and IV, The H. C. Ørsted Institute, DK 2100 Copenhagen, Denmark

Nickel Complexes of Thiohydrazonates. 3.[1,2] Crystal and Molecular Structures of [2,4-Pentanedione bis(thioacethydrazonato)]nickel(II)–Acetonitrile Adduct, Tetrabutylammonium [2,4-Pentanedione bis(thioacethydrazonato)]nickelate(II), and [Pentanetrione 2,4-bis(thioacethydrazonato)]nickel(II)

J. GABEL, V. HASEMANN, H. HENRIKSEN, ERIK LARSEN,* and SINE LARSEN*

Received July 26, 1978

The crystal structures of the three related nickel thiohydrazonate complexes indicated in the title have been studied by single-crystal X-ray crystallography. The parent compound, [2,4-pentanedione bis(thioacethydrazonato)]nickel(II), crystallizes as an acetonitrile adduct, I, in the monoclinic space group $P2_1/c$, with a = 22.671 (14) Å, b = 7.253 (5) Å, c = 17.359 (12) Å, β = 112.90 (4)°, and Z = 8. This compound is an acid and the corresponding base has been crystallized as a tetra-*n*-butylammonium salt. This latter compound, II, crystallizes in the monoclinic space group $P2_1/c$ with a = 21.662 (3) Å, b = 8.7604 (9) Å, c = 16.427 (3) Å, β = 101.49 (2)°, and Z = 4. The complex formed by air oxidation of the acid or the anion is a thiohydrazonate complex, III, derived from 2,3,4-pentanetrione and it crystallizes in the triclinic space group $P\bar{1}$, a = 7.567 (3) Å, b = 9.957 (4) Å, c = 10.939 (5) Å, α = 123.09 (2)°, β = 107.47 (2)°, γ = 91.19 (3)°, and Z = 2. The structures contain planar nickel(II) complexes with similar coordination of the nickel atoms. The acetonitrile molecules in I are disordered. The two crystallographically independent molecules in I have similar molecular dimensions, but they do not have as high a symmetry as the complexes in II and III both of which have an effective twofold axis of symmetry. The bond lengths in the acetylacetone part of the ligand in the structures of I and II are similar, indicating that I is present in a dipolar tautomeric form. This result is supported by ^{1}H NMR measurements. A comparison is given of the molecular dimensions of the structures internally and of related compounds. Finally the observed color differences between the three structures, of which I and II are red and III is green, are discussed in terms of simple MO theory.

Introduction

It has been known that molecules with the general formulas

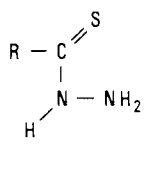

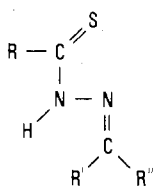

are able to act as chelate ligands for transition-metal ions since the pioneering work by Jensen.[3,4] Best known are the complexes of thiosemicarbazide and thiosemicarbazones which have attracted interest for a number of reasons. Thus some free ligands and their copper(II) complexes have been found to be biologically active in several ways.[5] Nickel(II) complexes of thiosemicarbazides and thiosemicarbazones are structurally very varied; in addition to planar four-coordinated complexes of both cis and trans sulfur arrangements,[6,7] there are also known complexes with five-[8] and six-coordination.[9,10] Nickel(II) complexes of dithiosemicarbazones of diketones have been found to undergo reversible redox reactions with the normal potentials of one-electron transfer reactions showing a systematic variation with the substituents.[11] In this con-

0020-1669/79/1318-1088$01.00/0